

# L-cut splitting of translation surfaces and non-embedding of pseudo-Anosovs (in genus two)

Andrew Bouwman and Jaroslaw Kwapisz

Department of Mathematical Sciences  
Montana State University  
Bozeman MT 59717-2400  
jarek@math.montana.edu  
[www.math.montana.edu/~jarek/](http://www.math.montana.edu/~jarek/)

April 18, 2016

## Abstract

We introduce a concept of a pair of parallel L-cuts on a translation surface, conjecture existence of such pairs for surfaces of genus  $g > 1$ , and find them for  $g = 2$ . We discuss applications to genus reducing decomposition of surfaces and to pseudo-Anosov maps (concerning their abelian-Nielsen equivalence classes and non-embedding into toral automorphisms). In particular, we provide a negative answer to the question about injectivity of the Abel-Franks map for genus two pseudo-Anosovs with orientable foliations.

# 1 Introduction

This introduction is divided into subsections, of which the first talks about existence of parallel L-cuts on translation surfaces and the following three discuss the implications. (At the end we describe the organization of the rest of the paper.)

## 1.1 Parallel L-cuts

Let  $M$  be a compact two dimensional surface carrying on the complement of a finite set  $M_{\text{sing}}$  an atlas of charts onto open subsets of the Cartesian  $(x, y)$ -plane  $\mathbb{R}^2$  with the transition functions that are translations. We additionally assume that the area of  $M$  is finite and the omitted points are conical singularities with angle  $2k\pi$  for  $k \in \{2, 3, \dots\}$ . Such  $M$  is called a *translation surface*.

The curvature of  $M$  is concentrated at the singularities, and the Gauss-Bonnet theorem gives the Euler characteristic of  $M$  as

$$\chi(M) = \sum_{z \in M_{\text{sing}}} -k(z) + 1. \quad (1.1)$$

For instance, for  $M$  of genus  $g = 2$  we have  $\chi(M) = 2 - 2g = -2$  and the sum is either  $-1 - 1$  or  $-2$ . This gives either two singularities with angle  $4\pi$  each or one singularity with angle  $6\pi$ . We denote the corresponding collections of surfaces by  $\mathcal{H}(1, 1)$  and  $\mathcal{H}(2)$ .

Any translation surface can be presented by identifying (via translations) pairs of parallel sides of a (connected and simple) polygon  $\mathcal{P}$  in  $\mathbb{R}^2$ . This fact, often taken as an elementary definition of translation surfaces, can be shown by using Veech's zippered rectangles [30] (reviewed in Section 4). In particular, for  $M$  in  $\mathcal{H}(2)$  and  $\mathcal{H}(1, 1)$  we shall use polygons  $\mathcal{P}$  that are octagons and decagons, respectively (Figures 4.1 and 4.3).

An oriented geodesic segment  $J$  in  $M$ , viewed locally in charts, yields straight segments in  $\mathbb{R}^2$  of some fixed direction recorded as the usual polar angle  $\theta \in [0, 2\pi)$ . We refer to such  $J$  simply as a *segment* and say that  $J$  is a *horizontal segment* if  $\theta \in \{0, \pi\}$  or a *vertical segment* if  $\theta \in \{\pi/2, 3\pi/2\}$ . (The attributes *up* or *down* and *left* or *right* have the obvious meaning.)

Segments with singularities at both ends and otherwise free of singularities are referred to as *saddle connections*. We shall call  $M$  *vh-simple* iff  $M$  has no vertical or horizontal saddle connections. For the most part, we restrict our discussion to vh-simple surfaces because this simplifies the statements, and such are the pseudo-Anosov surfaces in our main application (Section 1.3).

The central concept of this paper is that of an *L-cut* in  $M$ , by which we understand an oriented curve  $K$  in  $M$  that traces a finite vertical segment followed by a finite horizontal segment. If  $M$  is of genus  $g > 1$ , we additionally require that each end of  $K$  is a singular point. (The two ends may coincide.) Note that we allow  $K$  to have self-intersections or non-endpoint singularities. (This will not be the case

for the very  $K$  we construct for vh-simple  $M$  but may be unavoidable in general, cf. [4].)

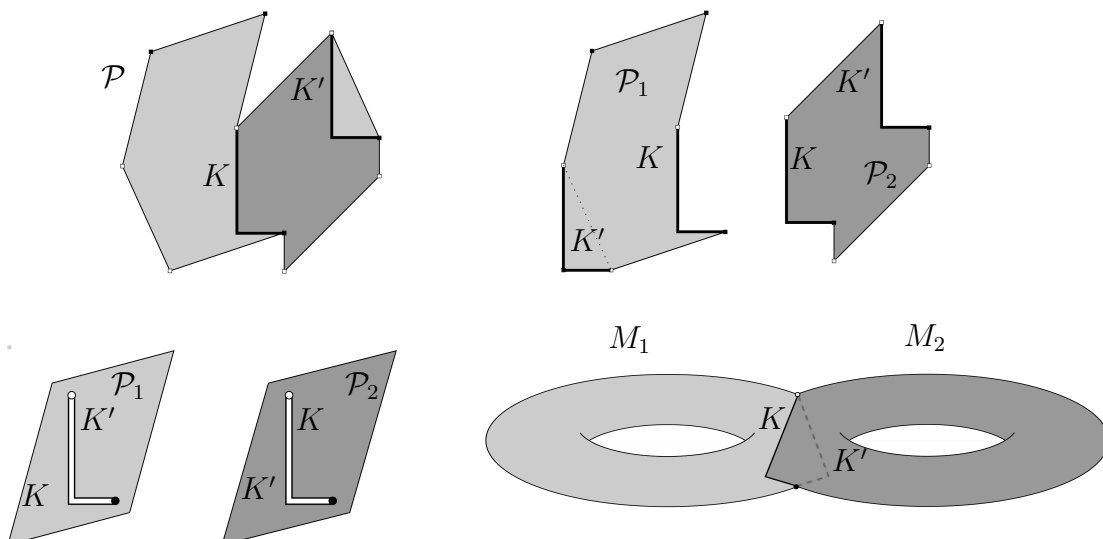


Figure 1.1: A surface  $M \in \mathcal{H}(1, 1)$  with a pair of parallel L-cuts  $(K, K')$ . The polygon  $\mathcal{P}$  presenting  $M$  decomposes into parts  $\mathcal{P}_1$  and  $\mathcal{P}_2$ , each presenting a subsurface of  $M$  with boundary  $K'K^{-1}$ . Since each of  $\mathcal{P}_1$  and  $\mathcal{P}_2$  can be rearranged into a parallelogram with a slit,  $M$  decomposes into a connected sum of tori  $M_1$  and  $M_2$  joined along L-cut slits.

A pair of L-cuts  $(K, K')$  is called *parallel* iff the two cuts begin at the same point and end at the same point and the loop  $K'K^{-1}$  (obtained by concatenating  $K'$  and the reverse of  $K$ ) is null-homologous. (See the upper left corner in Figure 1.1 for an example.) Observe that the homological condition guarantees that the horizontal segments of  $K$  and  $K'$  are of the same length  $h \geq 0$  and the vertical segments are of the same length  $v \geq 0$ . Indeed, if  $\omega$  is the closed complex 1-form on  $M$  given in the  $(x, y)$  coordinates (near regular points) by  $dx + idy$ , then vanishing of the homology class  $[K'K^{-1}]$  gives

$$\int_K \omega = \int_{K'} \omega,$$

where the complex number  $w := \int_K \omega$  (called the *holonomy vector* of  $K$ ) yields  $|\operatorname{Re}(w)| = h$  and  $|\operatorname{Im}(w)| = v$ . There are four possibilities for the signs of  $\operatorname{Re}(w)$  and  $\operatorname{Im}(w)$ , which we refer to as the *shape* of the L-cut  $K$ . (For  $-+$ ,  $K$  is L-shaped; for  $++$ ,  $K$  is  $\Gamma$ -shaped, etc.) Note that parallel L-cuts are of the same shape, and they can always be made L-shaped upon flipping the vertical/horizontal directions (i.e. postcomposing the charts with  $(x, y) \mapsto (\pm x, \pm y)$ ).

One of our main goals is to put forth the following conjecture.

**Conjecture 1.1** (L-cut Conjecture). *For any translation surface  $M$  of genus  $g > 1$ , there exists a pair of parallel L-cuts  $(K, K')$ .*

The core difficulty of the conjecture is retained (while skirting distracting degeneracies) under an additional hypothesis that  $M$  is vh-simple. For genus two, we have the following theorem, which is the main result of this paper.

**Theorem 1.2** (Existence of L-cuts). *For a vh-simple translation surface  $M$  of genus 2, there exists a pair of parallel L-cuts  $(K, K')$ . If  $M \in \mathcal{H}(1, 1)$  (and thus has two singularities), then each  $K$  and  $K'$  is a simple arc (i.e., a closed segment in  $\mathbb{R}$  embedded in  $M$ ) and its endpoints are at distinct singularities. If  $M \in \mathcal{H}(2)$  (and thus has one singularity), then each  $K$  and  $K'$  is a simple loop (i.e., a circle embedded in  $M$ ) through the singularity. In any case,  $K$  and  $K'$  do not intersect (at a point other than a singularity).*

It is worth noting that, if one restricts to *generic* translation surfaces, the conjecture has a quick proof by considerations employing the classical moduli space consisting of translation surfaces up to isomorphism (isometry that is a translation when viewed in charts). Indeed, any of the finitely many connected components of the moduli space (e.g.,  $\mathcal{H}(2)$  and  $\mathcal{H}(1, 1)$  for  $g = 2$ ) contains a surface  $M_0$  with a pair of homologous vertical saddle connections [8]. Thus the subset of the component consisting of the  $M$  with a pair of parallel L-cuts is non-empty (as it obviously contains all small perturbations of  $M_0$ ). This subset is open and manifestly invariant under the Teichmüller flow (which acts by postcomposing charts with  $(x, y) \mapsto (e^{t/2}x, e^{-t/2}y)$ ). By the celebrated result in [30, 25], Teichmüller flow is ergodic on each component with respect to a certain natural measure that is positive on open sets. Parallel L-cuts exist then on every surface in the moduli space excepting a closed nowhere dense set of measure zero. What renders this useless for our purposes is that the translation surfaces of pseudo-Anosov maps (which are in the center of our interest) correspond to the periodic orbits of the Teichmüller flow, and it is plausible that some such orbits are contained in the exceptional set.

## 1.2 Splitting into Connected Sum

Our theorem and conjecture are related to the translation surface theoretic counterpart of the well know topological fact that any closed orientable topological surface is homeomorphic to a connected sum of tori. Indeed, suppose that  $(K, K')$  is a pair of parallel L-cuts joining singularities  $z_0$  and  $z_1$  in a translation surface  $M$ . For the time being assume that that  $z_0 \neq z_1$  and that both  $K$  and  $K'$  are simple arcs (as in Figure 1.1). Then cutting  $M$  along the null-homologous curve  $K'K^{-1}$  results in two disjoint surfaces  $M'_1$  and  $M'_2$ . Each  $M'_i$  retains a copy of the curve  $K'K^{-1}$  as its boundary. The points of that boundary come in pairs  $(p, p')$  where  $p \in K$  and  $p' \in K'$  are the same distance along their cut. Upon identifying all such pairs, the  $M'_1$  and  $M'_2$  yield two translation surfaces  $M_1$  and  $M_2$  (without boundary), the *offspring* of  $M$ . The angle about each of the conical singularities  $z_0$  and  $z_1$  gets divided between  $M_1$  and  $M_2$ . For instance, in Figure 1.1, each of the

two original  $4\pi$  angles (at  $z_0$  and  $z_1$ ) renders a  $2\pi$  angle in each of the offspring  $M_i$ . It follows that, if we measure the complexity of a translation surface  $M$  by

$$c(M) := -\chi(M) + \#M_{\text{sing}} = \sum_{z \in M_{\text{sing}}} k(z) \geq 0, \quad (1.2)$$

then the offspring have lower complexity:

$$c(M_i) \leq c(M) \quad (i = 1, 2). \quad (1.3)$$

In fact, when  $z_0 \neq z_1$  (as we temporarily assumed), the inequality is strict for both  $i = 1, 2$ . When  $z_0 = z_1$ , there is a pathology (explained below) allowing  $c(M_i) = c(M)$  for one of the  $i = 1, 2$ . In any case, simple induction shows that, if pairs of parallel L-cuts can always be found and the splitting process can be continued, it will terminate and the set of last offspring will consist of translation surfaces of complexity zero, a finite collection of tori.

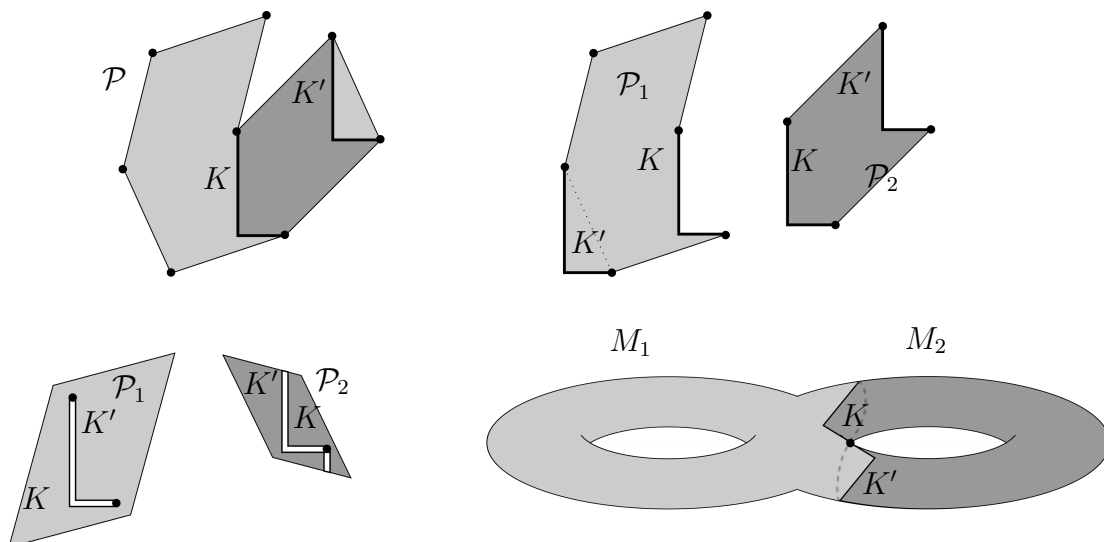


Figure 1.2: A surface  $M \in \mathcal{H}(2)$  with a pair of parallel L-cuts  $(K, K')$ . The polygon  $\mathcal{P}$  presenting  $M$  decomposes into two parts,  $\mathcal{P}_1$  and  $\mathcal{P}_2$ , each of which can be rearranged into a parallelogram with a slit. Note that  $\mathcal{P}_1$  inherits from  $\mathcal{P}$  the identification of the ends of the slit, which have to be disjoint to render  $M_1$  as a slitted torus.

The splitting when  $z_0 = z_1$  is less straightforward because we have four segments of  $K \cup K'$  meeting at  $z_0$ . Examining the identifications of these segments shows that  $z_0$  necessarily creates in one of the offspring  $M_i$  a pathology: a point with a neighborhood that consists of two disks joined at that point. One has to *disjoint* these disks to get a bona fide surface. (This disjointing increments the  $c(M_i)$ , allowing equality in (1.3).) The situation is depicted in Figure 1.2 where the two dots are the same in  $M$  but have to be treated as distinct in  $M_1$  for it to be a

torus. Only then, the L-cut becomes a simple arc in  $M_1$ . (It is a simple loop in  $M_2$ ).

The process of splitting  $M$  along the pair  $(K, K')$  of parallel L-cuts can be naturally reversed to present the original surface  $M$  as a version of the *connected sum construction* gluing two offspring surfaces along L-cut slits. In particular, we have the following corollary of Theorem 1.2.

**Corollary 1.3** (L-cut Connected Sum Theorem). *Any vh-simple genus two translation surface  $M$  is a connected sum of two tori  $M_1$  and  $M_2$  joined along isometric L-cuts,  $K_1$  in  $M_1$  and  $K_2$  in  $M_2$ . If  $M$  has two singularities then both  $K_1$  and  $K_2$  are simple arcs (as in Figure 1.1). If  $M$  has one singularity then  $K_1$  and  $K_2$  are a simple arc and a simple loop (as in Figure 1.2).*

The hypothesis of vh-simplicity can be certainly weakened (or even removed completely) at the cost of allowing pairs of L-cuts that are not simple arcs or loops, in which case formalizing the connected sum operation is more cumbersome. It would be too distracting to go in this direction here but Figure 1.3 illustrates one such generalized splitting. (Note the polygon presenting  $M_2$  has an *antenna* that carries important identification information.) A more complete treatment can be found in [4], where the vh-simplicity hypothesis is weakened to minimality of the vertical flow on  $M$ .

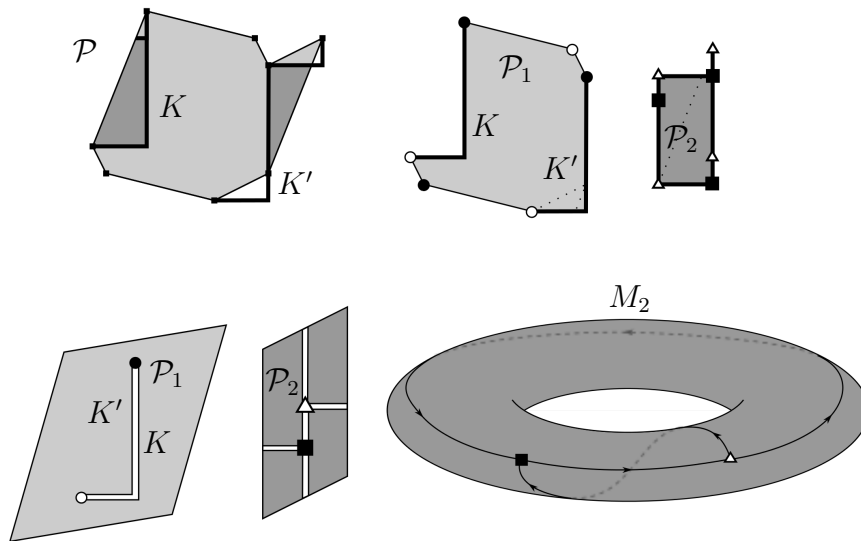


Figure 1.3: Splitting of  $M \in \mathcal{H}(2)$  along a pair of parallel L-cuts  $(K, K')$  with  $K'$  not a simple loop. While  $M_1$  is slit along simple L-cut,  $M_2$  is slit along a closed loop L-cut starting at the “triangle” and traversing twice the portion between the “square” and the “triangle” (the two points resulting from disjointing the singularity). This induces the “antenna” in the polygon  $\mathcal{P}_2$  presenting torus  $M_2$ .

Corollary 1.3 is analogous to the result of McMullen in [27] (see also [5]) asserting that any translation surface  $M$  can be rotated by some angle  $\theta$  to become a connected sum of two tori  $M_1$  and  $M_2$  joined along two vertical cuts,  $J_1$  in  $M_1$  and  $J_2$  in  $M_2$ . (Rotating  $M$  refers to changing the translation surface structure by postcomposing charts into  $\mathbb{R}^2$  with a rotation by  $\theta$ .) Although McMullen shows that there are infinitely many  $\theta$  facilitating such splitting, this does not seem to easily imply an L-cut splitting for  $\theta = 0$ .

Much is also known (see e.g. [21, 8]) about splitting of a *generic* translation surface along homologous saddle connections. This is used to catalog all connected components of the moduli space of translation surfaces but seems to have no immediate application to  $L$ -cut splitting for  $g > 2$ .

### 1.3 Non-embedding of surfaces into toral automorphisms

Recall that *toral automorphisms* are maps  $f_A : \mathbb{T}^N \rightarrow \mathbb{T}^N$  of the  $N$ -dimensional torus  $\mathbb{T}^N = \mathbb{R}^N / \mathbb{Z}^N$  conjugate to the map  $x \mapsto Ax \pmod{1}$  where  $A$  is an  $N \times N$  integer matrix of determinant  $\pm 1$ . (Here  $N > 1$  and  $\mathbb{Z}$  is the integers.) *Hyperbolic* toral automorphisms (*h.t.a.*) are distinguished by  $A$  having no eigenvalues of modulus one. They provide the simplest examples of diffeomorphisms exhibiting chaotic behavior.

By the device of Markov partitions [1, 28, 6], a h.t.a.  $f_A$  is measure theoretically isomorphic via a continuous a.e. injective map to a mixing Markov chain<sup>1</sup>. Therefore there is an uncountable zoo of compact  $f_A$ -invariant subsets of  $\mathbb{T}^N$ . The simplest subsets are the invariant subtori (which arise from rational  $A$ -invariant subspaces of  $\mathbb{R}^N$ ) and all the other are rather unwieldy in that they cannot even contain a rectifiable arc [24]. Hoping to generate some new interesting examples, one can ask about invariant subsets that are homeomorphic to a compact connected manifold  $M$  (of dimension greater than zero) other than a torus. This is the open question from the 1960s first discussed by Hirsch in [17]. Since the answer is an easy “no” for 1-dimensional  $M$ , the place to start is the case of 2-dimensional  $M$ .

This brings in another celebrated class of chaotic systems: the pseudo-Anosov maps. These were introduced by Thurston [29] in the 1970s in a development unrelated to Hirsch’s question. It is only through the prism of the results that came years later that we know that there is an intimate connection. Indeed, a h.t.a. is expansive and thus induces (as in the proof of Corollary 1.5 below) an expansive self-homeomorphism  $f : M \rightarrow M$  on any invariantly embedded subsurface  $M \subset \mathbb{T}^N$ , assuming such a surface exists. By a remarkable result (Theorem 1.6) proved independently by Lewowich [22] and Hiraide [16], such a homeomorphism  $f$  is necessarily a pseudo-Anosov map. What is more (Lemma 3.3), if that pseudo-

---

<sup>1</sup>These, in turn, are equivalent to Bernoulli shifts, measure theoretically [13] or even almost continuously [20]. Non-hyperbolic but ergodic toral automorphisms are also measure theoretically Bernoulli [19]; although, it is not known if that is true in the almost continuous (finitary) sense [23].

Anosov map has orientable stable/unstable foliations then the embedding has to coincide with the map  $h : M \rightarrow \mathbb{T}^N$  given by the very general  $\pi_1$ -stability theorem of Franks [12], first invoked in this context by Fathi [11]. (In the recent survey [14], Gromov calls  $h$  *Abel-Franks map*, after drawing a parallel with the classical Abel-Jacobi embedding of a Riemann surface.)

As we explain below, the map  $h$  is constructed by using the idea of global shadowing and is given by rather explicit power series (see e.g. [3]). It is locally injective on the complement of a finite set [11] and is often a.e. injective [3]. (So many pseudo-Anosov are indeed hiding inside hyperbolic toral automorphisms!)

To address Hirsch's question and show non-existence of an invariantly embedded  $M \subset \mathbb{T}^N$ , it suffices to prove non-injectivity of the Abel-Franks map  $h$ . This has been done so far only for a certain specific family of pseudo-Anosov maps with one singularity by Gavin Band in [2]. We add to this by showing that the scenario identified by Band is present in all surfaces of genus two. (The main advance is in dealing with  $M \in \mathcal{H}(1, 1)$ .) We prove the following.

**Theorem 1.4** (pA Non-Embedding Theorem). *Suppose that  $f : M \rightarrow M$  is a pseudo-Anosov map of a genus two surface with orientable foliations and  $f_A : \mathbb{T}^N \rightarrow \mathbb{T}^N$  is a hyperbolic toral automorphism. If  $\psi : M \rightarrow \mathbb{T}^N$  is continuous and such that  $\psi \circ f = \psi \circ f_A$ , then  $\psi$  is not injective.*

**Corollary 1.5.** *Suppose that  $M$  is a genus two surface and  $f_A : \mathbb{T}^N \rightarrow \mathbb{T}^N$  is a hyperbolic toral automorphism. If  $\psi : M \rightarrow \mathbb{T}^N$  is an embedding onto an  $f_A$ -invariant subset, then the map  $f := \psi^{-1} \circ f_A \circ \psi$  is a pseudo-Anosov map with non-orientable foliations.*

The corollary hinges on the following (already mentioned) result of Hiraide and Lewowicz

**Theorem 1.6** (Hiraide, Lewowicz). *Every expansive homeomorphism of a compact surface is conjugate to a pseudo-Anosov map (with orientable or non-orientable foliations).*

We suspect that no pseudo-Anosov map of any genus  $g > 1$ , whether the foliations are orientable or not, can be embedded into a h.t.a. However, a proof along our lines runs into sheer combinatorial and geometric complexity of pseudo-Anosov maps, which explodes rapidly with increasing genus.

## 1.4 Abelian-Nielsen non-separability of pseudo-Anosovs

Existence of parallel L-cuts has implications for Nielsen equivalence, a classical tool for classification and assignment of combinatorial data to periodic points of surface homeomorphisms. (For background, see Boyland's survey [7].)

Recall that two fixed points  $x$  and  $y$  of a homeomorphism  $f : M \rightarrow M$  are *Nielsen equivalent* iff there is an arc  $\gamma : [0, 1] \rightarrow M$  such that  $\gamma(0) = x$  and  $\gamma(1) = y$

and  $\gamma$  and  $f \circ \gamma$  are homotopic with fixed endpoints. ( $M$  being a surface, this is equivalent to saying that the loop  $f \circ \gamma \gamma^{-1}$  is null-homotopic.) We say that  $x$  and  $y$  are *abelian-Nielsen equivalent* iff an arc as above can be found but  $\gamma$  and  $f \circ \gamma$  are only homologous with fixed endpoints (i.e.  $f \circ \gamma \gamma^{-1}$  is hull-homologous).<sup>2</sup> To deal with periodic points of  $f$ , one applies the definitions to the iterates  $f^n$  ( $n \in \mathbb{N}$ ). It is well known (see Theorem 7.4 in [7]) that pseudo-Anosov maps are *Nielsen separating*, i.e., every fixed point of an iterate  $f^n$  ( $n \in \mathbb{N}$ ) of a pseudo-Anosov map  $f$  is the sole element of its Nielsen equivalence class. This is not the case when we replace *Nielsen* by *abelian-Nielsen*, and we have the following theorem.

**Theorem 1.7** (abelian-Nielsen non-separation). *Suppose that  $f$  is a pseudo-Anosov map  $f$  with orientable foliations on a surface of genus two. There are infinitely many  $n \in \mathbb{N}$  such that  $f^n$  has abelian-Nielsen equivalence classes that contain more than one fixed point of  $f^n$ .*

Again, we conjecture that the hypothesis on the genus can be dropped and abelian-Nielsen non-separation holds for all pseudo-Anosov maps.<sup>3</sup>

To get a better grasp of the theorem, let us interpret it in terms of the dynamics lifted to the universal cover  $\tilde{M}$  and to the homology cover  $\hat{M}$ . These covers are characterized by having deck groups equal to the fundamental group  $\pi_1(M)$  and the first homology  $H_1(M, \mathbb{Z})$ , respectively. ( $\hat{M}$ , which we will use extensively in Section 2, is also called the *maximal Abelian cover* of  $M$  on account of  $H_1(M, \mathbb{Z})$  being the abelianization of  $\pi_1(M)$ .) It is easy to see (cf. [7]) that Nielsen equivalence classes coincide with the fixed point sets of lifts of  $f^n$  to  $\tilde{M}$ , while abelian-Nielsen classes coincide with the fixed point sets of lifts of  $f^n$  to  $\hat{M}$ . To the extent that we have a deck group worth of such lifts and  $\pi_1(M)$  is much *bigger* than  $H_1(M, \mathbb{Z})$ , the theorem is very plausible.

As it stands, the proof of Theorem 1.7 (in Section 2) is a byproduct of a rather tedious construction of parallel L-cuts. Specifically, we identify two rectangles (Figure 2.1 in Section 2) on which some iterate  $f^n$  ( $n > 0$ ) is conjugate to the Smale's horseshoe. Because the L-cuts are homologous to each other, the periodic points (one from each horseshoe) with the same binary code are abelian-Nielsen equivalent to each other. (They will also be in the same fiber of the Abel-Franks map.) Such configuration of what we call *homologous horseshoes* first appeared in [2].

\*\*\*

Aware of the fact that readers interested in different aspects of our results may have different backgrounds, we include a good dose of expository material.

---

<sup>2</sup>The equivalence in [7] is a bit weaker to achieve its nice interpretation in the mapping cylinder of  $f$ .

<sup>3</sup>In such case, it would hold for all orientation preserving homeomorphisms  $f$  of surfaces that are irreducible aperiodic in Thurston's classification [10]. Such maps are homotopic to and *contain* all the dynamics of a certain pseudo-Anosov [15].

Sections 2 and 3 deal with pseudo-Anosovs. Section 2 explains how existence of L-cuts implies the non-embedding (Theorem 1.4) by combining the ideas of Franks, Fathi, and Band. It also shows the abelian-Nielsen non-separation (Theorem 1.7). Section 3 rounds the picture with some observations, including identification of any *would be* embedding as the Abel-Franks map.

Sections 4 and 5 collect tools from the theory of renormalization of translation surfaces. In Section 6, these tools are used to prove our main results on existence of L-cuts and splitting (Theorem 1.2 and Corollary 1.3), with the crux of the argument amounting to explicit elementary considerations of geometry of octagons and decagons.

## 2 Proof of non-embedding

The main goal of this section is establishing the non-embedding and the abelian-Nielsen non-separation theorems (Theorems 1.4 and 1.7). We follow the path blazed by Band [2] and centered on the global-shadowing characterization of the fibers of the *would be* embedding  $\psi : M \rightarrow \mathbb{T}^N$  (i.e., the map in Theorem 1.4). Unlike Band we do not assume at the outset that  $\psi$  is the Abel-Franks map, as first constructed by Fathi in [11] (see also [3]). However, the arguments readily adapt to this more general setting.

Suppose that  $f : M \rightarrow M$  is a continuous map of compact orientable surface,  $f_A : \mathbb{T}^N \rightarrow \mathbb{T}^N$  is a hyperbolic toral automorphism (induced by a matrix  $A$ ), and  $\psi : M \rightarrow \mathbb{T}^N$  is continuous such that

$$\psi \circ f = f_A \circ \psi. \tag{2.1}$$

At this point we do not assume yet that  $f$  is pseudo-Anosov with orientable foliations.

The main idea is to look at the situation at the level of homology covers,  $\hat{M}$  for  $M$  and  $\mathbb{R}^N$  for  $\mathbb{T}^N$ . The first integral homology  $H_1(M, \mathbb{Z})$  acts as the deck group of the covering  $\pi : \hat{M} \rightarrow M$ , and we write  $\hat{p} + v$  for the result of  $v$  acting on  $\hat{p}$ . Keep in mind that  $\hat{M}$  is an unbounded surface that (as a metric space) *coarsely resembles* the discrete group  $H_1(M, \mathbb{Z}) \simeq \mathbb{Z}^{2g}$  because the quotient  $\hat{M}/H_1(M, \mathbb{Z})$  is compact (equals  $M$ ). Even more concretely, one can think about  $\hat{M}$  as smoothly embedded into  $\mathbb{R}^{2g}$  as a  $\mathbb{Z}^{2g}$ -periodic surface on which  $H_1(M, \mathbb{Z})$  acts by integer translations. (The embedding is done by integrating harmonic 1-forms representing a basis of the cohomology; and the quotient embedding  $M \rightarrow \mathbb{T}^{2g}$  is the classical Abel-Jacobi map we mentioned before.)

The first step is to lift the maps  $f, \psi, f_A$  to  $\hat{f} : \hat{M} \rightarrow \hat{M}, \hat{\psi} : \hat{M} \rightarrow \mathbb{R}^N, \hat{f}_A : \mathbb{R}^N \rightarrow \mathbb{R}^N$ . These lifts are unique only up to deck transformations. In particular,  $\hat{f}_A$  is of the form  $p \mapsto Ap + \text{const}$ . It is convenient to adjust the lifts and conjugate  $\hat{f}_A$  by a suitable translation so that  $\hat{f}_A(p) = Ap$  and (2.1) becomes

$$\hat{\psi} \circ \hat{f} = A \circ \hat{\psi}. \tag{2.2}$$

To perform the adjustment, note that (2.1) gives  $\hat{\psi} \circ \hat{f} = \hat{f}_A \circ \hat{\psi} + u$  for some  $u \in \mathbb{Z}^N$ . That is  $\hat{\psi} \circ \hat{f} = \hat{f}'_A \circ \hat{\psi}$  if we take  $\hat{f}'_A := T_u \circ \hat{f}_A$  where  $T_u$  is the translation  $p \mapsto p + u$ . Because  $A$  is hyperbolic,  $\hat{f}'_A$  is conjugate by a translation to the linear transformation  $p \mapsto Ap$ , i.e.,  $\hat{f}'_A = T_{-s} \circ A \circ T_s$  for some  $s \in \mathbb{R}^N$ . Now, (2.2) holds upon replacing  $\hat{\psi}$  by  $T_{-s} \circ \hat{\psi}$ .

The key to studying the injectivity of  $\psi$  is the following implication (cf. Lemma 2.2 in [2]).

$$\forall_{\hat{x}, \hat{y} \in \hat{M}} \sup_{n \in \mathbb{Z}} \text{dist} \left( \hat{f}^n(\hat{x}), \hat{f}^n(\hat{y}) \right) < +\infty \implies \hat{\psi}(\hat{x}) = \hat{\psi}(\hat{y}). \quad (2.3)$$

Above, "dist" refers to any fixed equivariant metric on  $\hat{M}$ , say the one induced by lifting some Riemannian metric on  $M$ . The points  $\hat{x}$  and  $\hat{y}$  for which the supremum in (2.3) is finite are said to *globally shadow* each other.

The proof of (2.3), given below, starts with the simple insight that, to the extent that  $\hat{M}$  coarsely resembles  $H_1(M, \mathbb{Z}) \simeq \mathbb{Z}^{2g}$ , the lift  $\hat{\psi}$  can be viewed (see (2.4)) as a bounded perturbation of the map  $\psi_* : H_1(M, \mathbb{Z}) \rightarrow H_1(\mathbb{T}^N, \mathbb{Z}) \simeq \mathbb{Z}^N$  induced by  $\psi$  on the first homology.

*Proof of (2.3):* For any  $\hat{x} \in \hat{M}$ , by the definition of the induced map  $\psi_*$  we can write

$$\hat{\psi}(\hat{x}) = \hat{\psi}(\hat{x} - v) + \psi_* v \quad (\forall v \in H_1(M, \mathbb{Z})) \quad (2.4)$$

where  $\hat{x} - v$  is the result of the homology class  $-v$  acting on  $\hat{x}$ . Now,  $v$  can be selected to *approximate*  $\hat{x}$  in the sense that  $\hat{x} - v$  is in some, fixed once and for all, pre-compact fundamental domain for the action of  $H_1(M, \mathbb{Z})$ . Because the first term in (2.4) is bounded and the second linear, one easily concludes that  $\hat{\psi}$  is *Lipschitz at large scales*, i.e., there is  $\Lambda > 0$  so that

$$|\hat{\psi}(\hat{x}) - \hat{\psi}(\hat{x}')| \leq \Lambda + \Lambda \text{dist}(\hat{x}, \hat{x}') \quad (\forall \hat{x}, \hat{x}' \in \hat{M}). \quad (2.5)$$

(To get (2.5), use  $|\hat{\psi}(\hat{x}) - \hat{\psi}(\hat{x}')| \leq \Lambda_1 + \Lambda_2 |v - v'|$  and  $|v - v'| \leq \Lambda_3 \text{dist}(\hat{x}, \hat{x}')$ .)

Thus if  $C \geq 0$  is the supremum in (2.3), we have

$$\sup_{n \in \mathbb{Z}} \left| A^n \circ \hat{\psi}(\hat{x}) - A^n \circ \hat{\psi}(\hat{y}) \right| = \sup_{n \in \mathbb{Z}} \left| \hat{\psi} \circ \hat{f}^n(\hat{x}) - \hat{\psi} \circ \hat{f}^n(\hat{y}) \right| \leq \Lambda + \Lambda C < +\infty.$$

By hyperbolicity of  $A$ ,  $\sup_{n \in \mathbb{Z}} |A^n z| < \infty$  iff  $z = 0$  so (taking  $z := \hat{\psi}(\hat{x}) - \hat{\psi}(\hat{y})$ ) we get  $\hat{\psi}(\hat{x}) = \hat{\psi}(\hat{y})$ .  $\square$

**Remark 2.1.** *If  $\psi_*$  is additionally 1-1, the inverse of the implication in (2.3) can be obtained by reversing the argument above. If  $\psi_*$  is not 1-1, one can replace  $\hat{M}$  by a smaller covering  $\check{M} := \hat{M} / \ker \psi_*$  and then (using the requisite lifts  $\check{f}$  and  $\check{\psi}$  such that  $A \circ \check{\psi} = \check{\psi} \circ \check{f}$ ) the implication (2.5) turns into an equivalence:*

$$\forall_{\check{x}, \check{y} \in \check{M}} \sup_{n \in \mathbb{Z}} \text{dist} \left( \check{f}^n(\check{x}), \check{f}^n(\check{y}) \right) < +\infty \iff \check{\psi}(\check{x}) = \check{\psi}(\check{y}).$$

Moreover,  $\psi(x) = \psi(y)$  iff  $\check{\psi}(\check{x}) = \check{\psi}(\check{y})$  for some lifts  $\check{x}, \check{y} \in \check{M}$  of  $x, y$ .

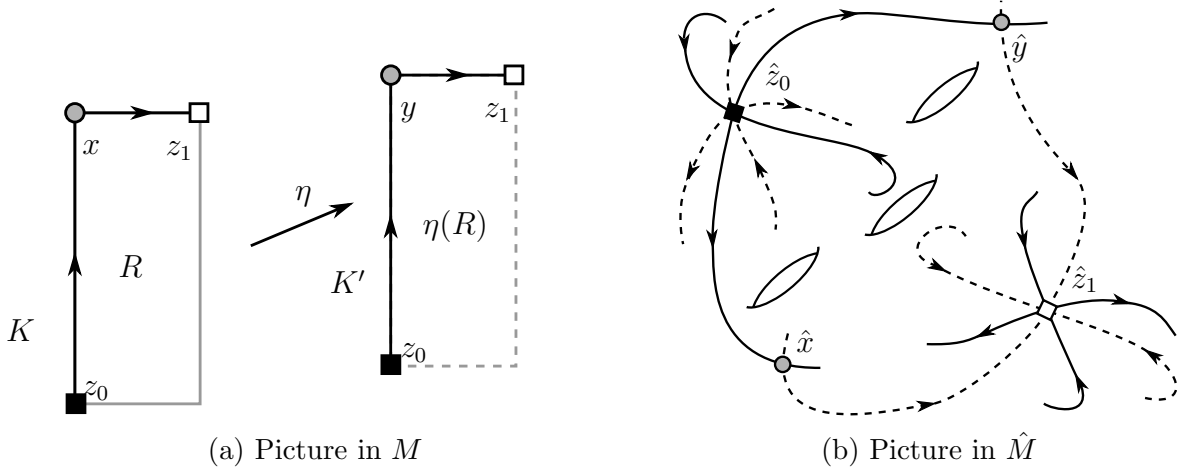


Figure 2.1: (Left:) Each of the turning points  $x \in K$  and  $y \in K'$  is a heteroclinic point at a transverse intersection of stable (horizontal) and unstable (vertical) manifolds of conical singularities  $z_0$  and  $z_1$ . (Right:) The situation in the lift to  $\hat{M}$  with  $4\pi$ -singularities  $\hat{z}_0, \hat{z}_1$  whose stable/unstable manifolds are depicted with solid lines and dashed lines, respectively. Crucially,  $\hat{x}$  and  $\hat{y}$  are heteroclinic to  $\hat{z}_0, \hat{z}_1$  because  $K$  and  $K'$  are homologous.

*Conclusion of Proof of Theorem 1.4:* Now we additionally assume that  $f$  is pseudo-Anosov with orientable foliations. It is well known (from [18]) that  $M$  can be turned into a Riemann surface so that the orientable stable/unstable measured foliations of  $f$  are the level lines of a holomorphic one-form. This form, in turn, defines a translation surface structure on  $M$  so that the unstable foliation is vertical and the stable foliation is horizontal (see e.g. [26]). Since every stable/unstable leaf of a pseudo-Anosov is dense (see e.g. [10]),  $M$  is vh-simple and we can invoke Theorem 1.2.

Let then  $(K, K')$  be a pair of L-cuts in  $M$  supplied by Theorem 1.2 and  $x \in K$  and  $y \in K'$  be the *turning points*, i.e., the non-endpoints where the horizontal and vertical segments meet (Figure 2.1b). The points  $x$  and  $y$  are *f-heteroclinic*, i.e.,  $x, y \in W^u(z_1) \cap W^s(z_0)$  (where  $W^{s/u}$  stand for the stable/unstable manifolds). Note that  $x \neq y$  since  $K \neq K'$ .

Crucially, the L-cuts are parallel, so the curve  $K'K^{-1}$  is null-homologous and thus lifts to a closed curve  $\hat{K}'\hat{K}^{-1}$  in  $\hat{M}$  (where  $\hat{K}$  and  $\hat{K}'$  are suitable lifts of  $K$  and  $K'$ ). In particular, the  $x, y$  lift to  $\hat{x}, \hat{y} \in \hat{M}$  that satisfy  $\hat{x}, \hat{y} \in W^u(\hat{z}_1) \cap W^s(\hat{z}_0)$ . Here the unstable/stable manifolds are with respect to the lifted map  $\hat{f}$  and the  $\hat{z}_i$  are lifts of the singularities. Although the  $\hat{z}_i$  need not be fixed by  $\hat{f}$ , the triangle inequality

$$\text{dist} \left( \hat{f}^n(\hat{x}), \hat{f}^n(\hat{y}) \right) \leq \text{dist} \left( \hat{f}^n(\hat{x}), \hat{f}^n(\hat{z}_i) \right) + \text{dist} \left( \hat{f}^n(\hat{z}_i), \hat{f}^n(\hat{y}) \right)$$

gives

$$\lim_{n \rightarrow \pm\infty} \text{dist} \left( \hat{f}^n(\hat{x}), \hat{f}^n(\hat{y}) \right) = 0 + 0 = 0. \quad (2.6)$$

By (2.3),  $\hat{\psi}(\hat{x}) = \hat{\psi}(\hat{y})$  and thus also  $\psi(x) = \psi(y)$ . Since  $x \neq y$ ,  $\psi$  is not injective.  $\square$

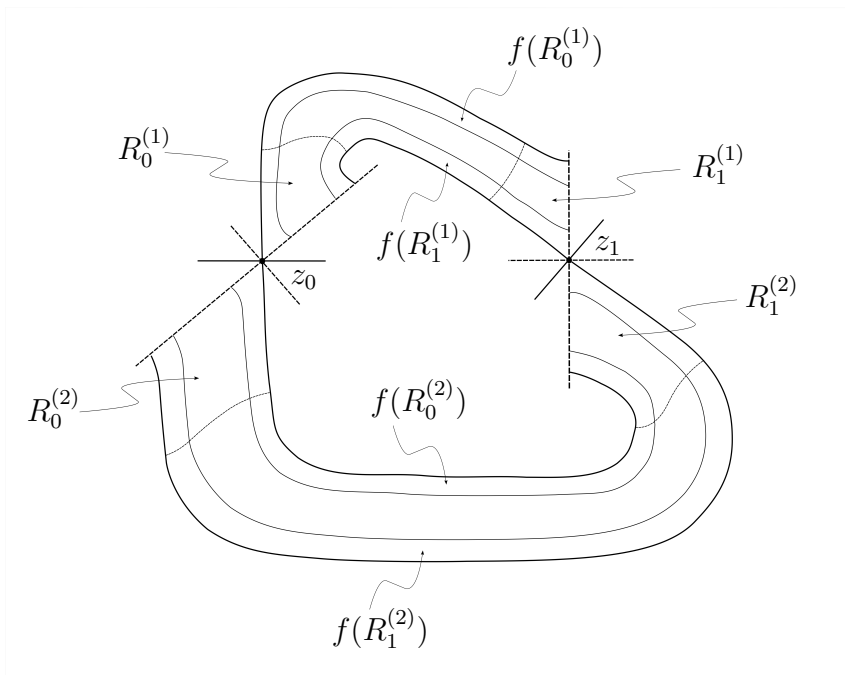


Figure 2.2: Two horseshoes in  $M$ : each rectangle  $R^{(i)}$  ( $i = 1, 2$ ) has subrectangles  $R_0^{(i)}$  and  $R_1^{(i)}$  mapping across  $R^{(i)}$  along the unstable manifolds (solid lines).

In fact, the injectivity of  $\psi$  fails in a rather decisive way as there is a whole Cantor set worth of distinct points identified by  $\psi$ :

**Theorem 2.2** (homologous horseshoes). *In the context of Theorem 1.4, there exist Cantor sets  $C_1, C_2 \subset M$  containing (each) all the singularities of  $M$  and there is a bijective relation  $C_1 \leftrightarrow C_2$  such that  $\psi(x) = \psi(y)$  for any pair  $(x, y)$  of related points. Moreover,  $f$  restricted to  $C_i$  is conjugate to the full shift on  $\{0, 1\}^{\mathbb{Z}}$  (for  $i = 1, 2$ ).*

To prove the theorem one can use the additional feature of the construction of parallel L-cuts in Section 6. Namely,  $K \cup \eta(K')$  bound a rectangle  $R^{(1)}$  in  $M$  and  $K' \cup \eta(K)$  bound a rectangle  $R^{(2)}$  in  $M$ . (In Figure 2.1a,  $R^{(1)} = R$  and  $R^{(2)} = \eta(R)$ .) In the language of [2], these rectangles are “horseshoe-like rectangles” that satisfy the hypotheses of Lemma 3.1 therein. The lemma gives the assertion of the theorem. What is happening is that each rectangle is mapped to itself in a horseshoe manner so that we have the usual Cantor sets,  $C_1 \subset R^{(1)}$  and  $C_2 \subset R^{(2)}$ ,

consisting of points whose bi-infinite orbits stay in their respective rectangle. The points of  $C_1$  and  $C_2$  are coded by binary sequences in  $\{0, 1\}^{\mathbb{Z}}$ , and the bijective relation  $C_1 \leftrightarrow C_2$  is that of having the same code, i.e.,  $x \in C_1$  and  $y \in C_2$  with the same code are identified by  $\psi$ ,  $\psi(x) = \psi(y)$ . In all this the fact that  $K$  and  $K'$  are homologous to each other is of critical importance and we refer to  $(C_1, C_2)$  as a pair of *homologous horseshoes*. The proof below gives a more precise account of Band's mechanism.

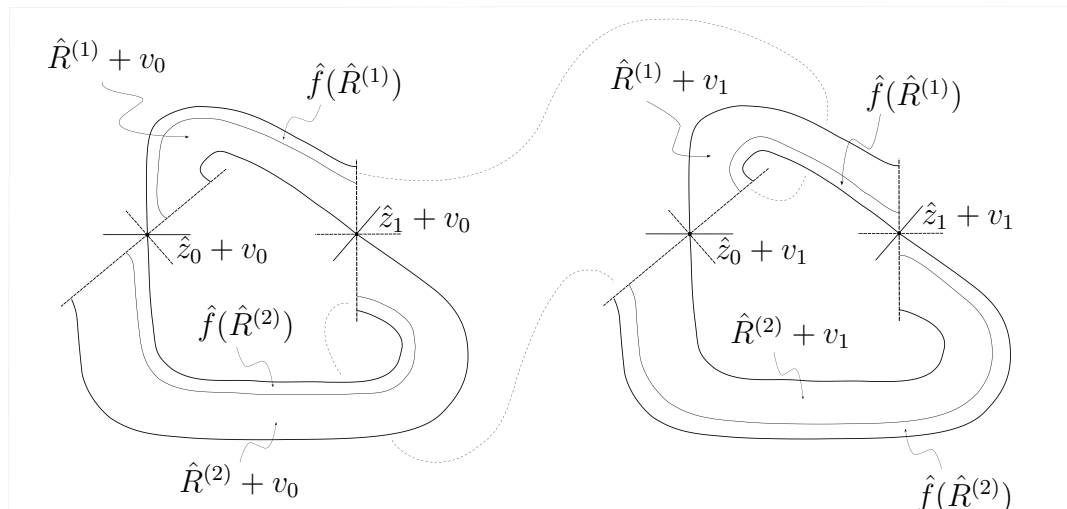


Figure 2.3: The horseshoes are homologous: the images of the lifted rectangles  $\hat{R}^{(i)}$  under  $\hat{f}$  stretch to connect lifted singularities  $\hat{z}_0 + v_0$  and  $\hat{z}_0 + v_1$  independent of  $i = 1, 2$ .

*Proof of Theorem 2.2.* First looking in  $M$  (Figure 2.2), we have the classical heteroclinic picture whereby  $f^{-1}(R^{(i)}) \cap R^{(i)}$  is a union of two disjoint subrectangles  $R_0^{(i)}$  and  $R_1^{(i)}$  of  $R^{(i)}$ , each *mapping across* the  $R^{(i)}$  under  $f$  (i.e.,  $f(R_j^{(i)})$  is a subrectangle traversing the whole  $R^{(i)}$  in the unstable direction).

Now, consider the situation in  $\hat{M}$  after lifting the rectangles  $R^{(i)}$  to rectangles  $\hat{R}^{(i)}$  in  $\hat{M}$  (Figure 2.3). Here we choose the lifts so that  $\hat{R}^{(1)}$  and  $\hat{R}^{(2)}$  have  $\hat{K}$  and  $\hat{K}'$  as a part of their boundary, respectively, where  $\hat{K}$  and  $\hat{K}'$  are as in the proof of Theorem 1.4 and Figure 2.1. (We also denote by  $\hat{R}_j^{(i)}$  the subrectangles of the  $\hat{R}^{(i)}$  that are the corresponding lifts of the  $R_j^{(i)}$ .) The lifts  $\hat{z}_j$  of  $z_j$  that are at the corners of the  $\hat{R}^{(i)}$  are not fixed by  $\hat{f}$  but merely satisfy  $\hat{f}(\hat{z}_j) = \hat{z}_j + v_j$  for some  $v_j \in H_1(M, \mathbb{Z})$ . Under  $\hat{f}$ ,  $\hat{R}_0^{(i)}$  maps across  $\hat{R}^{(i)} + v_0$ . In the process,  $\hat{R}_0^{(i)}$ 's subrectangles, denoted by  $\hat{R}_{00}^{(i)}$  and  $\hat{R}_{01}^{(i)}$ , map across  $\hat{R}_0^{(i)} + v_0$  and  $\hat{R}_1^{(i)} + v_0$ , respectively. Applying  $\hat{f}$  one more time maps  $\hat{R}_1^{(i)} + v_0$  across  $\hat{R}^{(i)} + f_*(v_0) + v_1$ . Note that  $f_*(v_0) + v_1$  does not depend on  $i = 1, 2$ . (The situation is similar for  $\hat{R}_{10}^{(i)}$  and  $\hat{R}_{11}^{(i)}$ .)

Extending this analysis beyond two iterates (as for the ordinary horseshoe), for every finite binary word  $\sigma = \sigma_1 \dots \sigma_m$ , we get a subrectangle  $R_\sigma^{(i)}$  whose points  $p$  have the *itinerary*  $\sigma$ , i.e., the first  $m+1$  iterates of  $p$ ,  $(f^k(p))_{k=0}^m$ , belong (successively) to the rectangles

$$R_{\sigma_1}^{(i)}, R_{\sigma_2}^{(i)}, \dots, R_{\sigma_m}^{(i)}, R^{(i)}.$$

The corresponding subrectangle  $\hat{R}_\sigma^{(i)}$  of  $\hat{R}^{(i)}$  has the  $m+1$  iterates of its points  $\hat{p}$  (successively) belonging to

$$\hat{R}_{\sigma_1}^{(i)}, \hat{R}_{\sigma_2}^{(i)} + v_{\sigma_1}, \dots, \hat{R}_{\sigma_m}^{(i)} + (f_*^{m-1}(v_{\sigma_1}) + \dots + v_{\sigma_{m-1}}), \hat{R}^{(i)} + (f_*^m(v_{\sigma_1}) + \dots + v_{\sigma_m}).$$

Again, the important detail is that the homology classes acting on to the rectangles  $\hat{R}_{\sigma_k}^{(i)}$  above do not depend on  $i = 1, 2$ . As a result, if  $\hat{x} \in \hat{R}_\sigma^{(1)}$  and  $\hat{y} \in \hat{R}_\sigma^{(2)}$ , then

$$\text{dist}(\hat{f}^k(\hat{x}), \hat{f}^k(\hat{y})) \leq 2 \max \left\{ \text{diam}(\hat{R}^{(1)}), \text{diam}(\hat{R}^{(2)}) \right\} \quad (k = 1, \dots, m).$$

A similar game is played with  $f$  replaced by  $f^{-1}$ . This shows that, if  $\hat{x}$  and  $\hat{y}$  have the same bi-infinite itineraries  $\sigma \in \{0, 1\}^{\mathbb{Z}}$ , then they globally shadow each other in  $\hat{M}$ . Thus, by (2.3),  $\hat{\psi}(\hat{x}) = \hat{\psi}(\hat{y})$  and so also  $\psi(x) = \psi(y)$ .  $\square$

By the way, the turning points  $x \in K$  and  $y \in K'$  used in the proof of Theorem 1.4 belong to the Cantors sets. They have itinerary  $\dots 0000000.111111 \dots$

Proof of Theorem 1.7. Let  $x \in R^{(1)}$  and  $y \in R^{(2)}$  be periodic points with the same itinerary. Take  $n \in \mathbb{N}$  to be a period (for both  $x$  and  $y$ ) so large that, denoting by  $\sigma$  the  $n$  long initial segment of the itinerary,  $\hat{R}_\sigma^{(i)}$  contains at most one lift for each fixed point of  $f^n$ . (This is possible because there is  $\epsilon > 0$  such that no two lifts of any point are closer than  $\epsilon$ , and  $\text{diam}(\hat{f}^{-n/2}(\hat{R}_\sigma^{(i)})) < \epsilon$  for large  $n$ .)

Let  $\hat{x} \in \hat{R}^{(1)}$  and  $\hat{y} \in \hat{R}^{(2)}$  by lifts of  $x$  and  $y$  as in the proof of Theorem 2.2. Because both  $x$  and  $y$  have the same itinerary, by the mechanism explained in the proof of Theorem 2.2, there is a common  $w \in H_1(M, \mathbb{Z})$  such that

$$\hat{f}^n(\hat{x}) \in R_\sigma^{(1)} + w \quad \text{and} \quad \hat{f}^n(\hat{y}) \in R_\sigma^{(2)} + w. \quad (2.7)$$

Since also  $\hat{x} \in R_\sigma^{(1)}$  and  $\hat{y} \in R_\sigma^{(2)}$  (due to the itinerary being an infinite concatenation of  $\sigma$ ), we have  $\hat{f}^n(\hat{x}) - w = \hat{x}$  and  $\hat{f}^n(\hat{y}) - w = \hat{y}$  by the choice of  $n$ .

We have shown that the map  $\hat{f}^n - w$  is a lift of  $f^n$  fixing both  $\hat{x}$  and  $\hat{y}$ . By the discussion in the introduction, this makes  $x$  and  $y$  abelian-Nielsen equivalent.  $\square$

### 3 Hirsch's embedding and Abel-Franks Map

For those interested in Hirsch's question, let us frame this open problem with a few observations that culminate in identification of the *would be* embedding  $\psi$  with an Abel-Franks map (Lemma 3.3). (This material is not used in our main proofs.)

As in the previous section, we suppose that  $f : M \rightarrow M$  is a homeomorphism of a compact surface,  $f_A : \mathbb{T}^N \rightarrow \mathbb{T}^N$  is a hyperbolic toral automorphism (induced by a matrix  $A$ ), and  $\psi : M \rightarrow \mathbb{T}^N$  is a continuous map for which the commutation (2.1) holds.

The first fact is that one may well assume that  $\psi$  induced map on homologies,  $\psi_* : H_1(M, \mathbb{R}) \rightarrow H_1(\mathbb{T}^N, \mathbb{R})$ , is surjective. To be precise, consider the image  $V := \psi_*(H_1(M, \mathbb{R}))$  in  $H_1(\mathbb{T}^N, \mathbb{R})$ . Upon identification  $H_1(\mathbb{T}^N, \mathbb{R}) \simeq \mathbb{R}^N$ , the  $f_A$  action on the homology coincides with the multiplication of column vectors in  $\mathbb{R}^N$  by the matrix  $A$ . By (2.1),  $V$  is an  $A$ -invariant subspace of  $\mathbb{R}^N$ . It contains  $\Gamma := \psi_*(H_1(M, \mathbb{Z}))$  as a lattice so that  $V/\Gamma$  is a subtorus of  $\mathbb{T}^N$ . The subtorus is  $f_A$ -invariant and  $f_A|_{V/\Gamma}$  is again a hyperbolic toral automorphism, specifically, it can be conjugated to  $f_{\tilde{A}} : \mathbb{T}^{\tilde{N}} \rightarrow \mathbb{T}^{\tilde{N}}$  where  $\tilde{N} := \dim V$  and  $\tilde{A}$  is an  $\tilde{N} \times \tilde{N}$  integer matrix representing  $A|_V$  in some integral basis of  $\Gamma$ . The following lemma allows one to restrict attention to the smaller torus  $\mathbb{T}^{\tilde{N}} \cong V/\Gamma$  and replace  $f_A$  by  $f_{\tilde{A}}$ . (It is a version of Theorem 3 in [17] with the fixed point assumption dropped.)

**Lemma 3.1** (Homological Containment).  $\psi(M) \subseteq V/\Gamma$ .

*Proof:* As in the previous section, we argue on the level of homology covers. In particular, we invoke (2.5) to see that  $\hat{\psi}(\hat{M})$  is contained in the  $\Lambda$ -neighborhood of  $V$ , making  $\hat{\psi}(\hat{M})/V$  a bounded subset of the quotient  $\mathbb{R}^N/V$ .  $\hat{\psi}(\hat{M})/V$  is also invariant under the  $A$ -induced automorphism of  $\mathbb{R}^N/V$ . Because this automorphism is hyperbolic  $\hat{\psi}(\hat{M})/V$  is just the origin  $\{0\}$ . Thus  $\hat{\psi}(\hat{M}) \subseteq V$ , which gives  $\psi(M) \subseteq V/\Gamma$ .  $\square$

The second item is the uniqueness of  $\psi$ , which goes back to Franks [12] and is considered in a much broader context in Gromov [14].

**Lemma 3.2** (Uniqueness). *If  $\psi'$  is another map  $M \rightarrow \mathbb{T}^N$  that satisfies the same hypotheses as  $\psi$  and acts in the same way on the first homology, i.e.,  $\psi_* = \psi'_*$ , then  $\psi = \psi'$ .*

*Proof:* For  $i = 1, 2, \dots, N$ , let  $\omega_i$  be a closed smooth form on  $M$  representing the singular cohomology class  $\psi^*[dx_i]$ . Take  $\hat{\omega}_i := \pi^*(\omega_i)$  to be the pull-back of  $\omega_i$  to  $\hat{M}$  via the covering  $\pi : \hat{M} \rightarrow M$ . By the key property of the homology cover  $\hat{M}$ , there are smooth functions  $\hat{\varphi}_i : \hat{M} \rightarrow \mathbb{R}$ ,  $i = 1, \dots, d$ , such that  $d\hat{\varphi}_i = \hat{\omega}_i$ . Set  $\hat{\Phi} := (\hat{\varphi}_1, \dots, \hat{\varphi}_N) : \hat{M} \rightarrow \mathbb{R}^N$ .

To finish the proof it suffices to show that  $\psi$  is characterized by the following *global shadowing property*:

$$\sup_{n \in \mathbb{Z}} \left| A^n \circ \hat{\psi}(\hat{x}) - \hat{\Phi} \circ \hat{f}^n(\hat{x}) \right| < +\infty \quad (\hat{x} \in \hat{M}). \quad (3.1)$$

Indeed, if  $\psi$  and  $\psi'$  act in the same way on the 1-st homology then they act in the same way on the 1-st cohomology. Hence  $\omega_i = \omega'_i$  and thus also  $\hat{\Phi} = \hat{\Phi}'$ . Invoking

(3.1) twice yields then

$$\sup_{n \in \mathbb{Z}} \left| A^n \circ \hat{\psi}(\hat{x}) - A^n \circ \hat{\psi}'(\hat{x}) \right| < +\infty \quad (\hat{x} \in \hat{M}). \quad (3.2)$$

Therefore  $\hat{\psi}(\hat{x}) = \hat{\psi}'(\hat{x})$ , again by the hyperbolicity of  $A$ .

To prove (3.1), taking  $\hat{x} \in \hat{M}$  and  $v \in H_1(M, \mathbb{Z})$ , we note that to get from  $\hat{\phi}_i(\hat{x})$  to  $\hat{\phi}_i(\hat{x} + v)$  one has to integrate  $\hat{\omega}_i$  along a smooth curve representing  $v$  (lifted to  $\hat{M}$ ) so that

$$\hat{\phi}_i(\hat{x} + v) = \hat{\phi}_i(\hat{x}) + \int_v \omega_i = \hat{\phi}_i(\hat{x}) + \int_v \psi^*[dx_i] = \hat{\phi}_i(\hat{x}) + \int_{\psi_* v} dx_i = \hat{\phi}_i(\hat{x}) + (\psi_* v)_i.$$

That is  $\hat{\Phi}$  satisfies

$$\hat{\Phi}(\hat{x} + v) = \hat{\Phi}(\hat{x}) + \psi_* v \quad (\hat{x} \in \hat{M}, v \in H_1(M, \mathbb{Z})). \quad (3.3)$$

This can be combined with (2.4), still selecting  $v \in H_1(M)$  with  $\hat{x} - v$  in some fixed pre-compact fundamental domain, to obtain

$$\left| \hat{\Phi}(\hat{x}) - \hat{\psi}(\hat{x}) \right| \leq |\hat{\Phi}(\hat{x} - v)| + |\hat{\psi}(\hat{x} - v)| \leq C$$

where  $C > 0$  is a constant independent of  $\hat{x}$  (courtesy of continuity of  $\hat{\Phi}$  and  $\hat{\psi}$ ). By using the commutation  $\hat{\phi} \circ \hat{f} = A \circ \hat{\phi}$  (from (2.2)), we obtain (3.1) as follows

$$\left| A^n \circ \hat{\psi}(\hat{x}) - \hat{\Phi} \circ \hat{f}^n(\hat{x}) \right| = \left| \hat{\psi} \circ \hat{f}^n(\hat{x}) - \hat{\Phi} \circ \hat{f}^n(\hat{x}) \right| \leq C.$$

□

Our third remark identifies  $\psi$  as the very Abel-Franks map  $h : M \rightarrow \mathbb{T}^N$  constructed by Fathi in [11]. (This is provided  $\psi_*$  is surjective, which can always be arranged via Lemma 3.1). To be specific, we refer to the description of the map  $h$  given in [3].

**Lemma 3.3.** *If  $\psi_* : H_1(M, \mathbb{R}) \rightarrow H_1(\mathbb{T}^N, \mathbb{R}) \cong \mathbb{R}^N$  is surjective then  $\psi$  coincides with the Abel-Franks map  $h : M \rightarrow \mathbb{T}^N$  constructed from a suitable set of cohomology classes.*

*Proof:* Define  $\Omega := \text{im } \psi^* = \text{span}_{\mathbb{R}}(\omega_1, \dots, \omega_N) \subset H^1(M, \mathbb{Z})$  where  $\omega_i := \psi^*[dx_i]$ , as before. Since  $f^* \circ \psi^* = \psi^* \circ f_A^*$  and  $\psi^*$  is injective,  $\Omega$  is  $f^*$ -invariant and the action of  $f^*$  on  $\Omega$  is conjugate to that of  $f_A^*$ . Let  $A_\Omega$  be the matrix of the linear transformation  $f^*|_\Omega$  with respect to the basis  $([\omega_1], \dots, [\omega_N])$ . The spectrum of  $A_\Omega$  is a subset of that of  $A^T$  (the matrix of  $f^*$ ), making  $A_\Omega$  hyperbolic. This means that the hypothesis (H) in [3] is satisfied allowing construction of the Abel-Franks map  $\hat{h} : \hat{M} \rightarrow \mathbb{R}^N$  with the  $\omega_1, \dots, \omega_N$  as the initial *ingredient 1-forms*. The quintessential property of this map is (see [3])

$$\sup_{n \in \mathbb{Z}} \left| A^n \circ \hat{h}(\hat{x}) - \hat{\Phi} \circ \hat{f}^n(\hat{x}) \right| < +\infty \quad (\hat{x} \in \hat{M}), \quad (3.4)$$

which is a version of global shadowing (3.2) with  $\hat{\phi}' := \hat{h}$ , so  $h$  coincides with  $\psi$  by the argument opening the proof of Lemma 3.2. □

## 4 Preliminaries on Veech's zippered rectangles

Our main result about existence of  $L$ -cuts (Theorem 1.2) depends on representation of translation surfaces by Veech's zippered rectangles [30]. In presence of nice introductory expositions in [31] and [32], a quick overview below should suffice.

We consider a translation surface  $M$  of genus two with no vertical saddle connections, which is the case when  $M$  is vh-simple. Let  $I \subset M$  be a horizontal segment whose left endpoint is a singular point of  $M$ . We will use  $I$  as a *cross-section* to the vertical flow on  $M$  proceeding vertically up with the unit speed. This flow is unambiguously defined, at least for short times, at non-singular points. At singularities one faces a choice of finitely many outgoing (up) or incoming (down) vertical segments to flow along. The absence of vertical saddle connections implies that the flow has no invariant proper sub-surfaces (with boundary) and thus is *minimal*, i.e., every infinite orbit is dense in all of  $M$ . In particular, the following hypothesis is satisfied.

(H1) Any point of  $M$  not in the outgoing vertical of a singularity hits  $I$  under the vertical flow in some negative time.

This hypothesis allows one to study  $M$  via the flow's first return map  $T : I \rightarrow I$  because  $M$  is filled by the flow's forward trajectories starting in  $I$ . (This is also true for backward trajectories; in fact, (H1) is preserved under the reversal of the direction of the flow.) Because the flow is area preserving, the first return  $T(x)$  of  $x$  is well defined for a.e. point  $x \in I$  by a general argument based on Poincaré recurrence theorem. In fact,  $T$  is an *interval exchange*, and its structure is dictated by  $M$  in a way detailed below.

First, consider  $M \in \mathcal{H}(2)$ . Let  $I'$  be  $I$  with endpoints removed. Each point of  $I'$  will either flow into a singularity or return to a unique point on  $I$ . As the sole singular point  $z_0$  has angle  $6\pi$ , there are three verticals incoming into  $z_0$  and (in absence of vertical saddle connections) there are exactly three different points  $p_1, p_2, p_3$  where these verticals first encounter  $I'$  under the backward flow, see Figure 4.1. The three points cut  $I'$  into four segments, labeled  $A, B, C$ , and  $D$ , with constant return times on each, denoted  $t_A, t_B, t_C$ , and  $t_D$ . Actually, this is not quite correct because we failed to account for the possible additional discontinuity of the return time at the point of  $I'$  which flows into the right endpoint of  $I$ . To avoid introducing one more cut at that point (and getting five segments), one adjusts the length of  $I$  (by moving its right endpoint) to secure the following additional hypothesis.

(H2) The right endpoint of  $I$  joins to a singularity by a vertical segment that does not intersect  $I$  at non-endpoints.

Under (H2),  $T : I \rightarrow I$  is an interval exchange map on exactly four segments  $A, B, C$ , and  $D$ . Denoting their respective lengths by  $\lambda_A, \lambda_B, \lambda_C$ , and  $\lambda_D$ , we see that  $M$  is a union of closures of four *open rectangles* swept by the segments. To be precise, the open rectangle associated to  $A$  is the subset of  $M$  that is a (locally)

isometrically immersed copy of the open  $\lambda_A \times t_A$  rectangle in  $\mathbb{R}^2$  obtained by flowing  $A$  for times in the interval  $(0, t_A)$ .

The decomposition of  $M$  into the four rectangles leads to a presentation of  $M$  as *Veech's zippered rectangle* consisting of two disjoint unions of closed rectangles in  $\mathbb{R}^2$ , each union having one rectangle with dimensions  $\lambda_A \times t_A$ ,  $\lambda_B \times t_B$ ,  $\lambda_C \times t_C$ , and  $\lambda_D \times t_D$ . The *upper union* has the rectangles positioned with the bases along a horizontal segment in  $\mathbb{R}^2$ , which we identify with  $I$ , and placed in their original order along  $I$  (Figure 4.1). The *lower union* has rectangles with their tops aligned along  $I$  in the order after application of the exchange  $T$ . Each of the two unions renders a translation surface isomorphic to  $M$  once the boundaries of the rectangles are subject to appropriate identifications (detailed in [30]). In a nutshell, the horizontal sides glue according to  $T$  (the top of the rectangle over  $A$  glues to  $T(A)$ , etc.) Glued are also the portions of the overlaying vertical sides before they reach a singularity (dashed in Figure 4.1). With a little work, one can now figure out the remaining identifications of the slits in the figure and the verticals over the right endpoint of  $I$ .

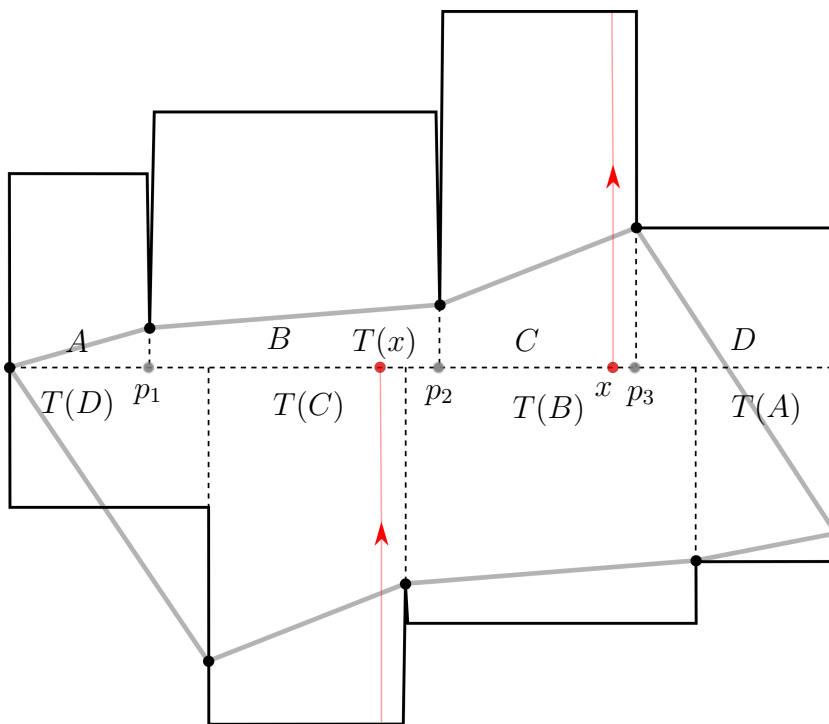


Figure 4.1: A zippered rectangle and an octagon representing  $M \in \mathcal{H}(2)$ .

In most instances, joining the points corresponding to singularities of  $M$  in the zippered rectangle yields a simple polygon  $\mathcal{P}$ , an octagon  $\mathcal{O}$  for  $M \in \mathcal{H}(2)$  (Figure 4.1). Taken with the obvious side identifications,  $\mathcal{P}$  gives a more intuitive presentation of  $M$ . We will avoid the situation, called *fishtail*, when  $\mathcal{P}$  is not a simple polygon (see Figure 4.2).

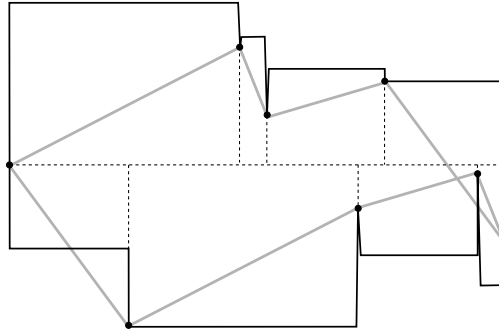


Figure 4.2: A zippered rectangle yielding a non-simple polygon with a *fishtail*.

All of the above discussion can be repeated for  $M \in \mathcal{H}(1,1)$  (see e.g. [5]). Roughly, the four verticals incoming into the two  $4\pi$  singularities  $z_0$  and  $z_1$  cut  $I$  into five segments, labeled  $A, B, C, D$ , and  $E$  (Figure 4.3). There are five rectangles per union and the polygon is a decagon, with the same fishtail caveat.

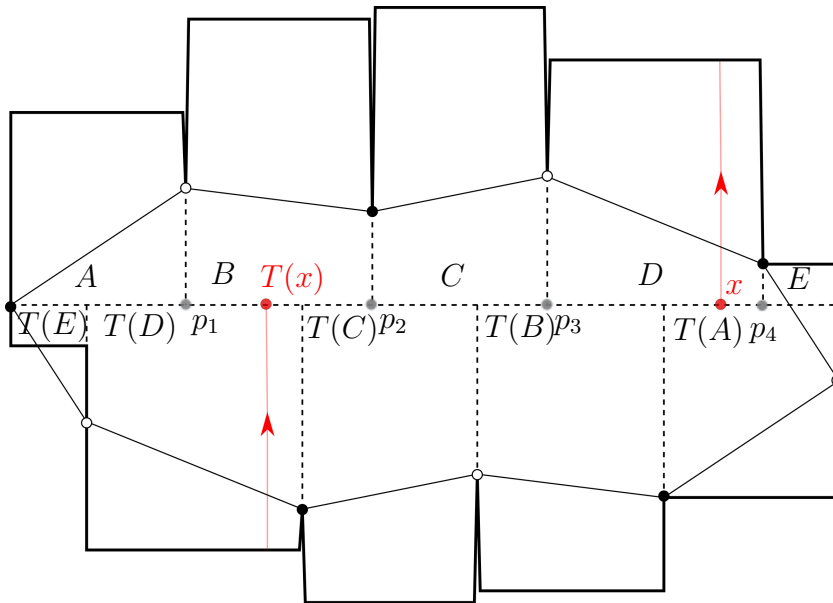


Figure 4.3: A zippered rectangle and a decagon representing  $M \in \mathcal{H}(1,1)$ .

## 5 Preliminaries on Rauzy-Veech diagrams

Still following [32] and [31], we review now *Rauzy-Veech operations* giving a way of transforming a zippered rectangle representing  $M$  into a new zippered rectangle representing the same  $M$  but with a shorter cross-section. This is done by looking at the rightmost segments among the pre- and post- $T$  segments and shrinking  $I$  by removing the shorter one, called the *loser*. The longer segment, called the *winner*, has its rightmost portion cut away accordingly, and so is cut the corresponding portion of the winner's rectangle. This portion and the whole rectangle of the loser are repositioned and reattached (within their upper/lower unions) so as to create a new zippered rectangle. This is best understood by looking at Figure 5.1 (Top), where  $D$  is the winner and  $T(A)$  is the loser. The operation is said to be of *type 0* if the winner is above the loser (as depicted) and of *type 1* otherwise (as would be the case if we flipped the figure upside down).

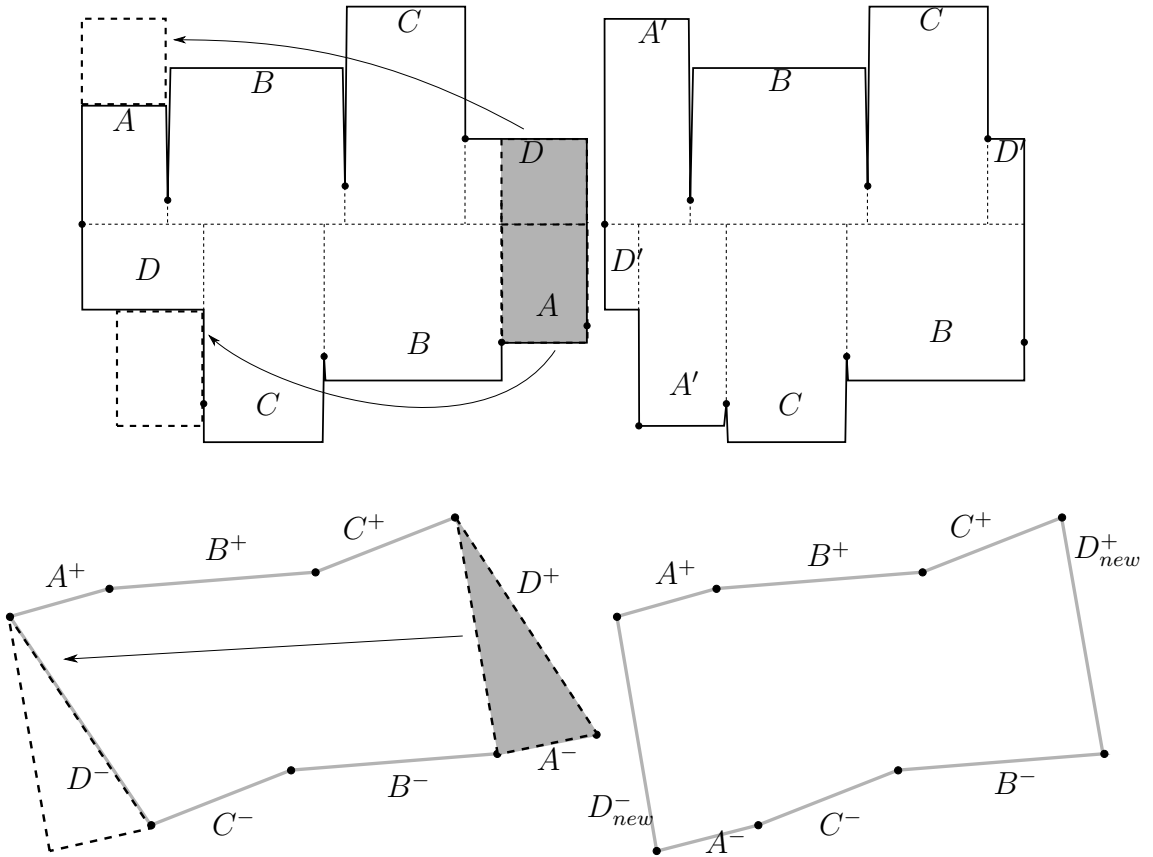


Figure 5.1: Type 0 operation for  $M \in \mathcal{H}(2)$ , on a zippered rectangle (Top) and on the octagon (Bottom). The datum changes from  $\begin{bmatrix} ABCD \\ DCBA \end{bmatrix}$  to  $\begin{bmatrix} ABCD \\ DACB \end{bmatrix}$ .

When the initial zippered rectangle does not fishtail and thus yields a polygonal

representation  $\mathcal{P}$  of  $M$  (Bottom of Figure 5.1), the Rauzy-Veech operation is a simple matter of cutting from  $\mathcal{P}$  the triangle spanned by the two rightmost sides and reattaching it at the bottom (type 0) or the top (type 1).

In any case, for a surface  $M$  without vertical saddle connections, starting with one zippered rectangle, Rauzy-Veech operation can be iterated to generate an **infinite sequence of zippered rectangles** (associated to  $M$  with a choice of a cross-section  $I$ ). The proof of Theorem 1.2 (in Section 6) will depend on this by carrying out geometric considerations on the zippered rectangles in this sequence with particularly simple combinatorial structure.

To this end, we will have to pay attention to the zippered rectangle's *combinatorial datum*, which can be read off of the associated interval exchange  $T : I \rightarrow I$  and consists of two finite sequences of segment labels arranged in the order of the segments before and after the application of  $T$  (cf. Figure 5.1). The Rauzy diagrams in Figures 5.2 and 5.3, depict all possible combinatorial data for zippered rectangles (coming from  $I$  satisfying hypotheses (H1,H2)) for  $M \in \mathcal{H}(2)$  and  $M \in \mathcal{H}(1,1)$ , respectively<sup>4</sup>. (The arrows indicate Rauzy operations.)

Note that reversing the vertical flow (i.e., replacing  $T$  by  $T^{-1}$ ) is responsible for the symmetry of the diagrams, with the caveat that it swaps the operation types 0 and 1 and turns each combinatorial datum upside-down. Our favorite is the node fixed by this symmetry, the *central node*. It is free of the fishtailing pathology and is always visited by the sequence, a fact we record in a separate lemma below.

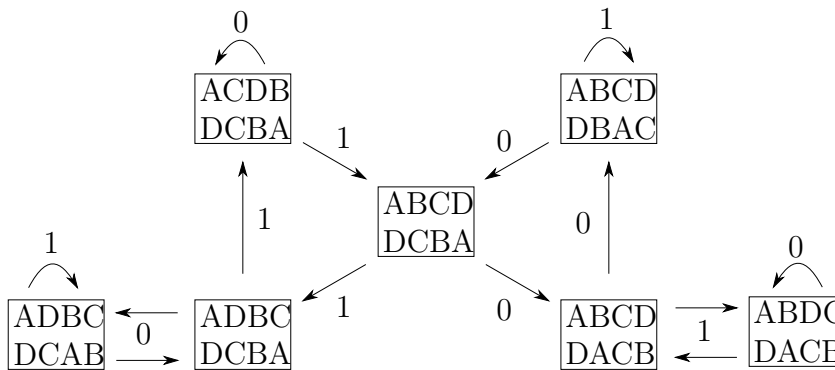


Figure 5.2: Rauzy diagram for the stratum  $\mathcal{H}(2)$ .

---

<sup>4</sup>Generally, there is a connected Rauzy diagram for each connected component of the moduli space of translation surfaces; see [30] and the discussions in [21] and [33].

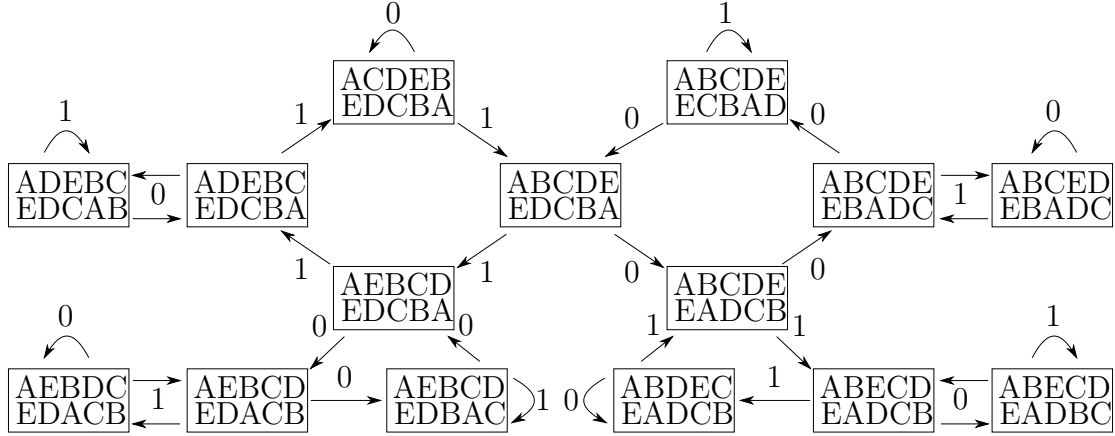


Figure 5.3: Rauzy diagram for the stratum  $\mathcal{H}(1,1)$ .

**Lemma 5.1.** *For  $M$  with no vertical saddle connections (with a choice of cross-section  $I$  satisfying (H1) and (H2)), the sequence of zippered rectangles associated to  $M$  necessarily visits the central node,  $\begin{bmatrix} ABCD \\ DCBA \end{bmatrix}$  if  $M \in \mathcal{H}(2)$  and  $\begin{bmatrix} ABCDE \\ EDCBA \end{bmatrix}$  if  $M \in \mathcal{H}(1,1)$ .*

*Proof:* Let  $M \in \mathcal{H}(2)$ . Every Rauzy operation shortens one of the segments  $A$ ,  $B$ ,  $C$ , or  $D$ . Proposition 4.3 in [32] states that, proceeding along the sequence, every segment gets shortened infinitely many times. As  $A$  is only shortened on the left half of the diagram and  $D$  is only shortened on the right half, we must pass through the central node.

For  $M \in \mathcal{H}(1,1)$ , the argument is similar.  $A$  is only shortened on the left half of the diagram and  $E$  is only shortened on the right half, so we must pass through the central node again by Proposition 4.3.  $\square$

## 6 Proof of Existence of L-cuts

In this section we prove Theorems 1.2 and 1.3. Due to Lemma 5.1, we assume that the vh-simple surface  $M$  has a zippered rectangle representation with combinatorial datum given by the central node (Section 5). Since this combinatorial type precludes fishtailing (Section 4), we will work with the polygonal presentation of  $M$ , an octagon for  $M \in \mathcal{H}(2)$  and a decagon for  $M \in \mathcal{H}(1,1)$  (Figures 4.1 and 4.3). Observe that these polygons are centrally symmetric. The central symmetry induces on  $M$  an isometric involution  $\eta : M \rightarrow M$  with six fixed points. This is the *Weierstrass involution* of  $M$  considered as a Riemann surface (see [9] and [5]). Note that  $\eta_* : H_1(M, \mathbb{R}) \rightarrow H_1(M, \mathbb{R})$  takes any homology class to its opposite, i.e.,  $\eta_* = -\text{Id}$ .

The overall strategy of the argument is to find in  $M$  a certain *rectangle*  $R$  (see Figure 2.1a). To be precise, if  $M \in \mathcal{H}(1, 1)$ , by a *rectangle* we mean a homeomorphic image of a closed rectangle in  $\mathbb{R}^2$  mapped into  $M$  via a local isometry preserving the horizontal and vertical directions. If  $M \in \mathcal{H}(2)$ , we allow identification of two diagonally opposite vertices, i.e., the map is continuous and 1-1 except for that identification. The reason for this is that our  $R$  will have a pair of opposite vertices at distinct singularities for  $M \in \mathcal{H}(1, 1)$  and at the sole singularity for  $M \in \mathcal{H}(2)$ . While the set of singularities is preserved by  $\eta$ , it will be key to ensure that

$$\eta(R) \neq R. \tag{6.1}$$

Indeed, if  $J$  is the saddle connection joining the opposite vertices of  $R$  and we choose an orientation on  $J$ , then (6.1) guarantees that  $\eta(J)J^{-1}$  forms a loop of distinct saddle connections in  $M$  whose homology class is fixed by  $\eta_*$  and thus is null. By taking a vertical and a horizontal side from each  $R$  and  $\eta(R)$  (as in Figure 2.1a), one forms distinct L-cuts  $K$  and  $K'$  that are homologous (actually homotopic) rel their endpoints to  $J^{-1}$  and  $\eta(J)$ , respectively. By this construction  $K^{-1}K'$  is null-homologous, making  $(K, K')$  a pair of parallel L-cuts exactly as asserted by Theorem 1.2. (In particular,  $K$  and  $K'$  are simple arcs or loops, as stipulated.) To establish Theorem 1.3, one has to additionally exhibit the decomposition of  $M$  for each instance of  $R$  we construct, which is easy (if a bit tedious).

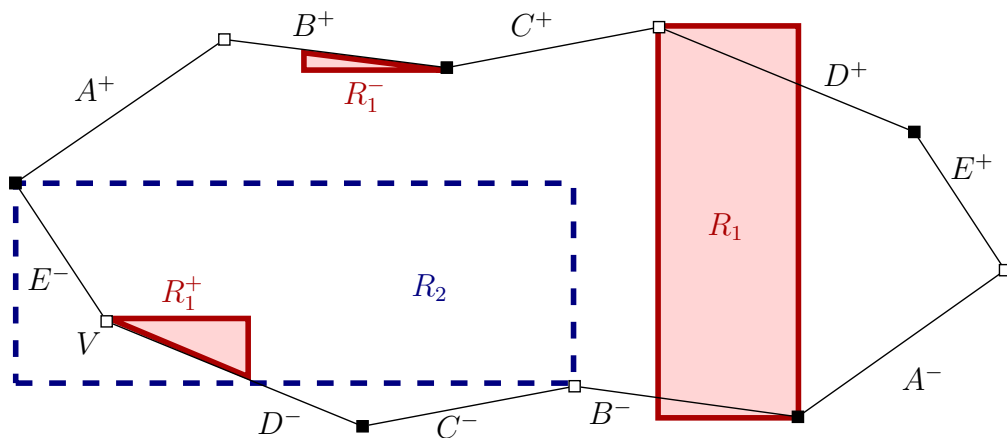


Figure 6.1: The candidate rectangle  $R_1$  has two triangular *protrusions* corresponding to the triangular regions  $R_1^+$  and  $R_1^-$  in the decagon  $\mathcal{D}$  (via the identifications of  $D^{+/-}$  and  $B^{+/-}$ , respectively).  $R_1$  is free of *invasions*, i.e., it encounters singularities only at its corners.  $R_1$  defines a rectangle in  $M$ . In contrast, the candidate rectangle  $R_2$  is invaded by the vertex  $V$  and fails to define a rectangle in  $M$ .

The rest of this section is devoted to finding a rectangle  $R$  in  $M$  with the desired properties. This will be done by taking a polygon  $\mathcal{P}$  representing  $M$  and considering up to five *candidate rectangles*,  $R_1, R_2, \dots$ , which are certain explicit Euclidean rectangles in the plane containing  $\mathcal{P}$ . We will examine each candidate

rectangle  $R_*$  to see if it defines a rectangle  $R$  in  $M$  under the tacit assumption that any protrusions of  $R_*$  (typically triangular) extending beyond  $\mathcal{P}$  are to be translated to the interior of  $\mathcal{P}$  according to the edge identifications (Figure 6.1). This process may fail to produce a rectangle  $R \subset M$  when the candidate rectangle  $R_*$  contains a vertex  $V$  of  $\mathcal{P}$  (thus placing a conical singularity inside  $R$ ). We will refer to such a situation as an *invasion* of  $R_*$  by  $V$ . (Figure 6.1 gives an example.) On the other hand, if  $R_*$  is not invaded then, as a matter of general principle, it produces  $R \subset M$  that is only an *immersed rectangle* (i.e., one with overlap). However, we shall see that  $R$  is in fact a bona fide rectangle in all instances we examine.

*Conclusion of Proof of Theorem 1.2 for  $M \in \mathcal{H}(2)$ :* As discussed, we present  $M$  by an octagon  $\mathcal{O}$  with combinatorial datum  $\begin{bmatrix} ABCD \\ DCBA \end{bmatrix}$ . We consider two candidate rectangles:  $R_1$ , with a diagonal homotopic to  $D + A$ , and  $R_2$ , with a diagonal homotopic to  $C + D + A$ ; both are depicted in Figure 6.2. Observe that neither of  $R_1$  and  $R_2$  is invariant under the central symmetry of  $\mathcal{O}$  so (6.1) is guaranteed. Our goal is to establish that, depending on  $\mathcal{O}$ , at least one of the rectangles  $R_1$  and  $R_2$  is free of invasion by a vertex and defines a rectangle in  $M$ . In the process, we may have to replace  $\mathcal{O}$  by the octagon (still with central node combinatorics) obtained by performing some Rauzy operations on  $\mathcal{O}$ .

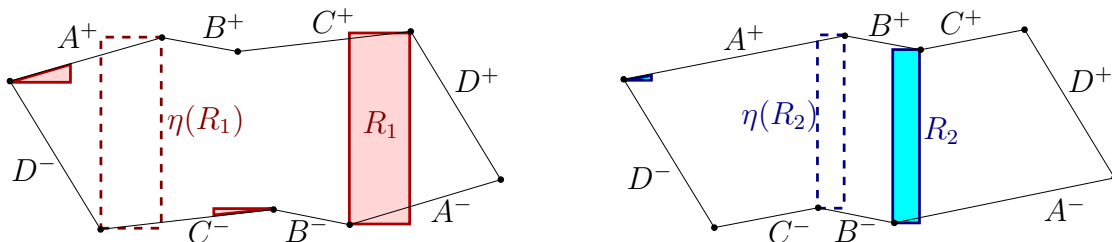


Figure 6.2: Candidate rectangles  $R_1$  and  $R_2$  for  $\mathcal{H}(2)$ .

For  $S \in \{A, B, C, D\}$ ,  $S^+$  denotes the upper edge of  $\mathcal{O}$  labeled  $S$ , i.e., the edge that came from the upper union in the zippered rectangle. Likewise,  $S^-$  denotes the lower edge of  $\mathcal{O}$  labeled  $S$ . We will refer to the segment length  $\lambda_S$  (Section 4), as the *width* of  $S^\pm$ . Since  $M$  has no vertical saddle connections  $\lambda_S > 0$  for all  $S$  and  $\lambda_A \neq \lambda_D$ ,  $\lambda_A \neq \lambda_C + \lambda_D$ , and  $\lambda_A \neq \lambda_B + \lambda_C + \lambda_D$ . Also, since there are no horizontal saddle connections in  $M$ , none of the edges of  $\mathcal{O}$  is horizontal.

It can be assumed that  $\lambda_A > \lambda_D$ , perhaps at the cost of reversing the direction of the vertical flow and relabeling the segments. Also, if  $\lambda_A > \lambda_B + \lambda_C + \lambda_D$ , then one can perform a sequence of three successive type 1 operations on  $\mathcal{O}$  (cf. Figure 5.2) and end back in the central node. Repeating this as many times as necessary yields  $\mathcal{O}$  for which  $\lambda_A < \lambda_B + \lambda_C + \lambda_D$ . Thus, the only remaining variability in  $\mathcal{O}$  we have to consider is whether  $\lambda_A$  is longer or shorter than  $\lambda_C + \lambda_D$ . Both cases are illustrated in Figure 6.3.

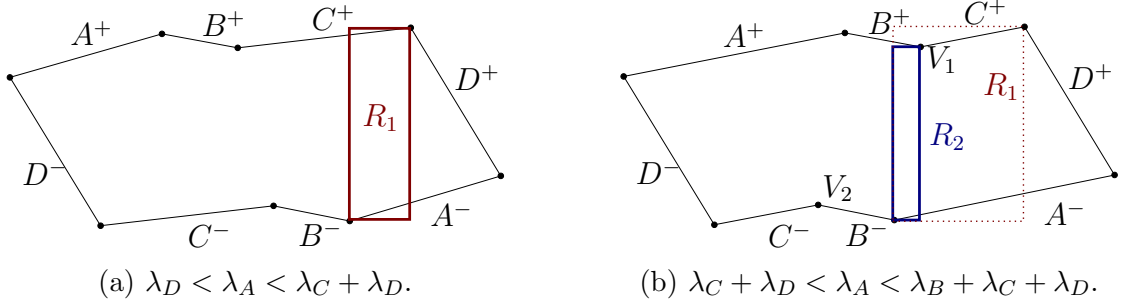


Figure 6.3: Representative diagrams for  $M \in \mathcal{H}(2)$  with  $\lambda_D < \lambda_A < \lambda_B + \lambda_C + \lambda_D$ .

*Case 1:*  $\lambda_D < \lambda_A < \lambda_C + \lambda_D$ . It is clear from Figure 6.3a, that no vertex can invade  $R_1$  and  $R_1$  defines a rectangle  $R$  in  $M$ .

*Case 2:*  $\lambda_C + \lambda_D < \lambda_A < \lambda_B + \lambda_C + \lambda_D$ . Look at Figure 6.3b. If  $C$  has a negative slope,  $R_1$  is still uninvaded and as in Case 1. Now, if  $C$  has positive slope, the vertex  $V_1$  at the left end of  $C^+$  invades  $R_1$ . However,  $V_2$  at the left end of  $B^-$  (which may have invaded  $R_2$  in Case 1) is now far enough to the left that  $R_2$  has no invasion and defines a rectangle  $R$  in  $M$ .  $\square$

*Conclusion of Proof of Theorem 1.3 for  $M \in \mathcal{H}(2)$ :* One has to exhibit a splitting of  $M$  into two genus one translation surfaces  $M_1$  and  $M_2$  for each of the two cases considered above. We leave it to the reader to sketch  $K$  and  $K'$  onto Figure 6.3 (cf. Figure 2.1a) and see that  $K$  and  $K'$  are essentially disjoint (i.e., only meet at the singularity). Then,  $K'K^{-1}$  being null-homologous guarantees that slicing  $\mathcal{O}$  along  $K$  and  $K'$  produces two polygons each yielding a translation surface  $M_i$  ( $i = 1, 2$ ). To be precise, this is only so after *disjointing* of two points, as discussed in the introduction. The  $M_i$  are tori (after the L-cut slits are closed) by the Euler characteristic argument from the introduction. (This can also be seen directly by drawing versions of Figure 1.1.)  $M$  is a connected sum of  $M_1$  and  $M_2$ , as asserted.  $\square$

*Conclusion of Proof of Theorem 1.2 for  $M \in \mathcal{H}(1, 1)$ :* As before, we present  $M$  as a decagon with combinatorial datum of the central node, this time  $\begin{bmatrix} ABCDE \\ EDCBA \end{bmatrix}$ . We consider 5 candidate rectangles depicted in Figure 6.4:  $R_1$  with a diagonal homotopic to  $D + E + A$ ,  $R_2$  with a diagonal homotopic to  $E + A + B$ ,  $R_3$  with a diagonal homotopic to  $A + B + C$ ,  $R_4$  with a diagonal homotopic to  $C + D + E$ , and  $R_5$  with a diagonal homotopic to  $B + C + D$ . Again, (6.1) is guaranteed and we have to show that, depending on  $\mathcal{D}$ , at least one of the rectangles  $R_1$  through  $R_5$  is free of invasion by a vertex of  $\mathcal{D}$  and defines a rectangle in  $R \subset M$ . To shorten the phrasing we shall refer to such candidate rectangles simply as *good*. We use that no edge  $S$  of  $\mathcal{D}$  can be horizontal,  $\lambda_S > 0$  for  $S \in \{A, B, C, D, E\}$ , and  $\lambda_A \neq \lambda_E$ ,  $\lambda_A \neq \lambda_D + \lambda_E$ ,  $\lambda_A \neq \lambda_C + \lambda_D + \lambda_E$ , and  $\lambda_A \neq \lambda_B + \lambda_C + \lambda_D + \lambda_E$ .

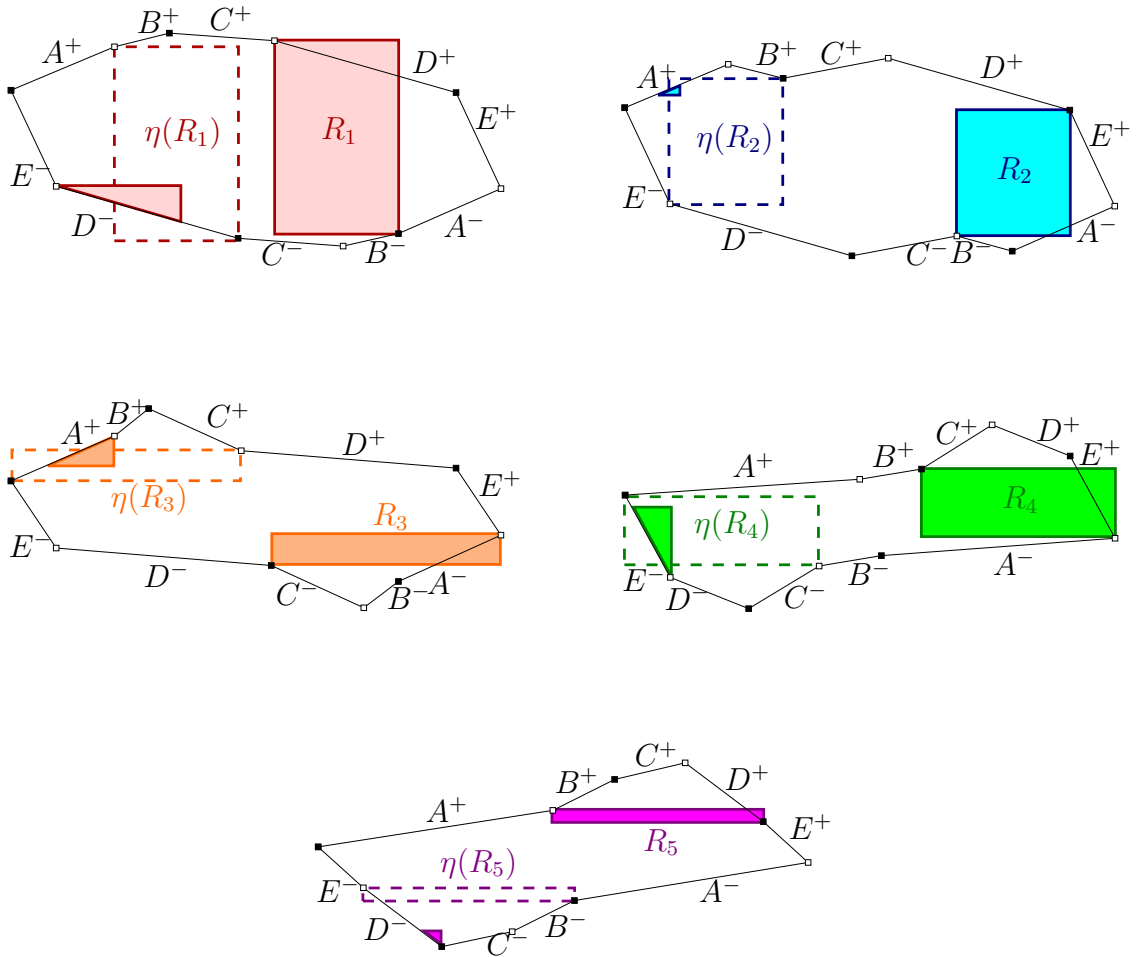


Figure 6.4: Candidate rectangles  $R_1$  through  $R_5$  for  $\mathcal{H}(1,1)$ .

As before, we assume  $\lambda_A > \lambda_E$ , after perhaps reversing the vertical flow and relabeling. Also, we can take that  $\lambda_A < \lambda_B + \lambda_C + \lambda_D + \lambda_E$ , as otherwise one can transform  $\mathcal{D}$  by a sequence of 4 consecutive type 1 operations (cf. Figure 5.3) until  $\mathcal{D}$  satisfies this inequality.

This leaves 3 major cases for  $\mathcal{D}$ , again arranged by the relative length of  $\lambda_A$  compared to sums of other lengths. (Cases 1 and 2 are depicted in Figure 6.5 and Case 3 is depicted in Figure 6.6.)

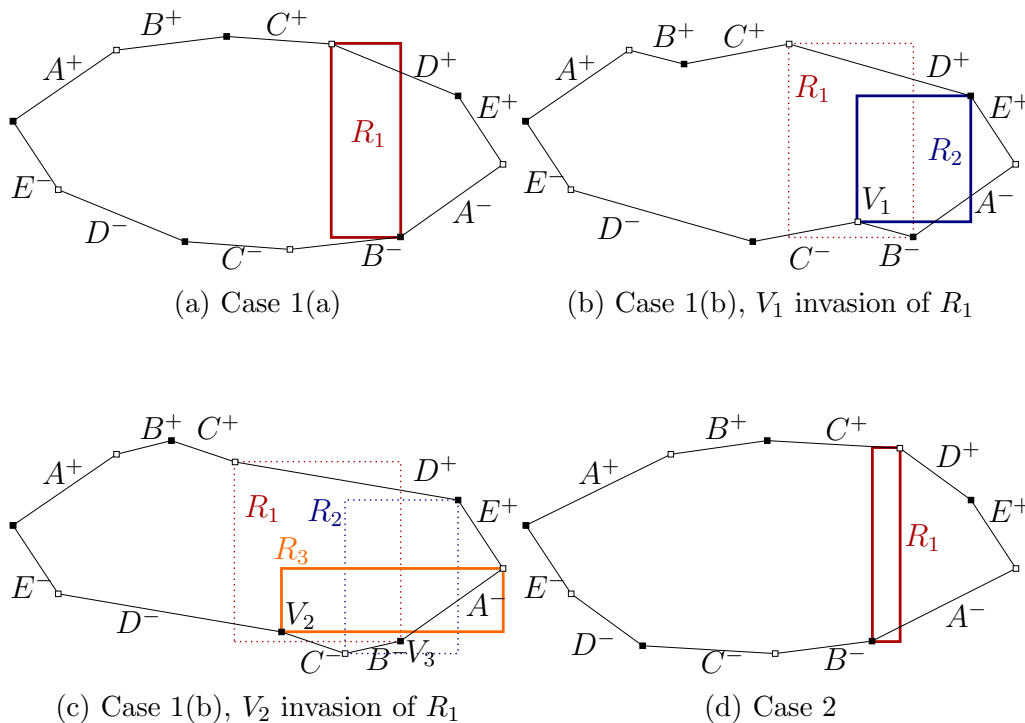


Figure 6.5: Representative diagrams for  $\mathcal{H}(1,1)$ , cases 1 ( $\lambda_E < \lambda_A < \lambda_D + \lambda_E$ ) and 2 ( $\lambda_D + \lambda_E < \lambda_A < \lambda_C + \lambda_D + \lambda_E$ ).

*Case 1:*  $\lambda_E < \lambda_A < \lambda_D + \lambda_E$ .

- Subcase (a),  $\lambda_A + \lambda_B > \lambda_D + \lambda_E$ :  $R_1$  is clearly *good*.
- Subcase (b),  $\lambda_A + \lambda_B < \lambda_D + \lambda_E$ : We may well assume that  $R_1$  is not *good*. Two vertices can invade  $R_1$ : If  $B$  has negative slope, the vertex  $V_1$  at the left end of  $B^-$  invades  $R_1$ . However, in this case  $R_2$  is *good*. Assuming now  $B$  has positive slope (and  $R_2$  is invaded), another possibility is that the vertex  $V_2$  at the left end of  $C^-$  invades  $R_1$ , but by doing so it must be higher than the vertex  $V_3$  at the right end of  $B^-$ , making  $R_3$  free of invasion.

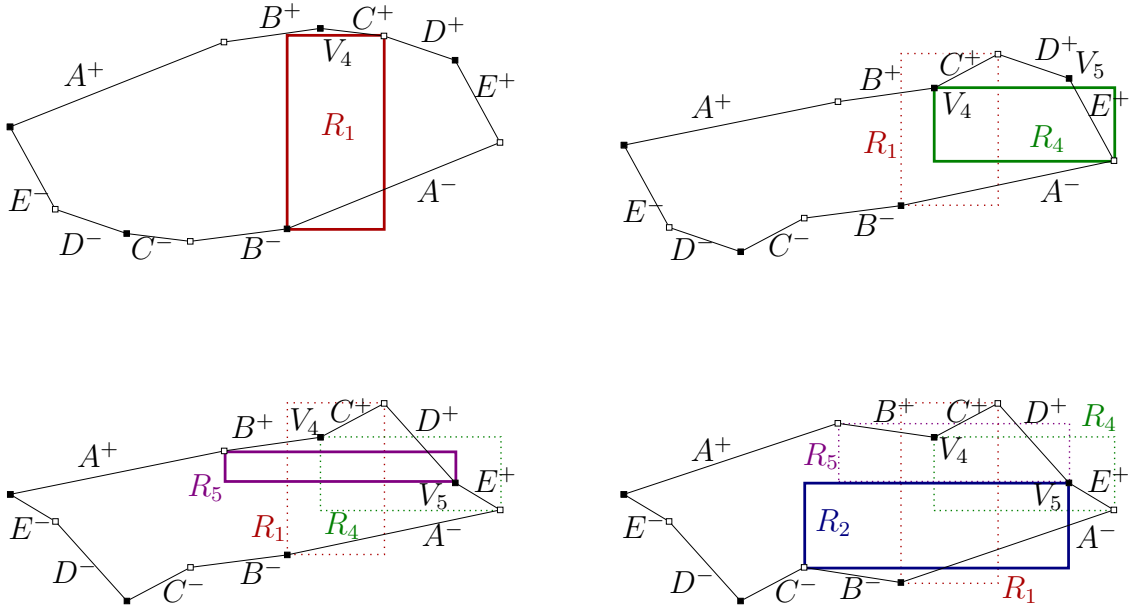


Figure 6.6: Representative diagrams for  $\mathcal{H}(1,1)$ , case 3 ( $\lambda_C + \lambda_D + \lambda_E < \lambda_A < \lambda_B + \lambda_C + \lambda_D + \lambda_E$ ).

*Case 2:*  $\lambda_D + \lambda_E < \lambda_A < \lambda_C + \lambda_D + \lambda_E$ .  $R_1$  is *good*.

*Case 3:*  $\lambda_C + \lambda_D + \lambda_E < \lambda_A < \lambda_B + \lambda_C + \lambda_D + \lambda_E$ .

- Subcase (a),  $C$  has negative slope: the vertex  $V_4$  at the left endpoint of  $C^+$  will be above  $R_1$ . So  $R_1$  has no invasion and it is *good*.
- Subcase (b),  $C$  has positive slope and the vertex  $V_5$  at the right end of  $D^+$  stays above  $V_4$ :  $R_4$  is *good*.
- Subcase (c),  $C$  has positive slope and  $V_5$  drops below  $V_4$ , and  $B$  has positive slope:  $V_5$  invades  $R_4$  but does not invade  $R_5$ . Since  $B$  has positive slope,  $V_4$  does not invade  $R_5$ .  $R_5$  is *good*.
- Subcase (d), as in (c) but  $B$  has negative slope:  $R_2$  is clearly *good*.

□

*Conclusion of Proof of Theorem 1.3 for  $M \in \mathcal{H}(1,1)$ :* As for  $M \in \mathcal{H}(2)$ , one has to see that  $K$  and  $K'$  are essentially disjoint, which can be done already by looking at Figure 6.4, or by inspecting Figures 6.5 and 6.6 for each of the individual cases. Thus we have a null-homologous simple loop  $K'K^{-1}$  that cuts  $M$  into two translation surfaces  $M_1$  and  $M_2$ , as in Figure 1.1. Again, by the Euler characteristic argument from the introduction (or direct laborious inspection), the  $M_i$  are tori (with L-cut slits). □

## References

- [1] Roy L. Adler and Benjamin Weiss. *Similarity of automorphisms of the torus*. Memoirs of the American Mathematical Society, No. 98. American Mathematical Society, Providence, R.I., 1970.
- [2] Gavin Band. Identifying points of a pseudo-Anosov homeomorphism. *Fund. Math.*, 180(2):185–198, 2003.
- [3] Marcy Barge and Jaroslaw Kwapisz. Hyperbolic pseudo-Anosov maps almost everywhere embed into a toral automorphism. *Ergodic Theory Dynam. Systems*, 26(4):961–972, 2006.
- [4] Andrew Bouwman. *L-cuts for genus two translation surfaces*. PhD thesis, Montana State University, 2013.
- [5] Andrew Bouwman and Jaroslaw Kwapisz. Young person’s guide to translation surfaces of genus two: McMullen’s connected sum theorem. *Rocky Mountain J. Math.*, 43(1):37–53, 2013.
- [6] Rufus Bowen. Markov partitions for Axiom A diffeomorphisms. *Amer. J. Math.*, 92:725–747, 1970.
- [7] Philip Boyland. Topological methods in surface dynamics. *Topology Appl.*, 58(3):223–298, 1994.
- [8] Alex Eskin, Howard Masur, and Anton Zorich. Moduli spaces of abelian differentials: the principal boundary, counting problems, and the Siegel-Veech constants. *Publ. Math. Inst. Hautes Études Sci.*, 97:61–179, 2003.
- [9] H. M. Farkas and I. Kra. *Riemann surfaces*, volume 71 of *Graduate Texts in Mathematics*. Springer-Verlag, New York, second edition, 1992.
- [10] A. Fathi, F. Laudenbach, and V. Poenaru. *Travaux de Thurston sur les surfaces*. Société Mathématique de France, Paris, 1991. Séminaire Orsay, Reprint of it *Travaux de Thurston sur les surfaces*, Soc. Math. France, Paris, 1979 [MR0568308 (82m:57003)], Astérisque No. 66-67 (1991).
- [11] Albert Fathi. Some compact invariant sets for hyperbolic linear automorphisms of tori. *Ergodic Theory Dynam. Systems*, 8(2):191–204, 1988.
- [12] John Franks. Anosov diffeomorphisms. In *Global Analysis (Proc. Sympos. Pure Math., Vol. XIV, Berkeley, Calif., 1968)*, pages 61–93. Amer. Math. Soc., Providence, R.I., 1970.
- [13] N. A. Friedman and D. S. Ornstein. On isomorphism of weak Bernoulli transformations. *Advances in Math.*, 5:365–394 (1970), 1970.
- [14] M. Gromov. Super stable Kählerian horseshoe? In *Essays in mathematics and its applications*, pages 151–229. Springer, Heidelberg, 2012.

- [15] Michael Handel. Global shadowing of pseudo-Anosov homeomorphisms. *Ergodic Theory and Dynamical Systems*, 5:373–377, 9 1985.
- [16] Koichi Hiraide. Expansive homeomorphisms of compact surfaces are pseudo-Anosov. *Osaka J. Math.*, 27(1):117–162, 1990.
- [17] Morris W. Hirsch. On invariant subsets of hyperbolic sets. In *Essays on Topology and Related Topics (Mémoires dédiés à Georges de Rham)*, pages 126–135. Springer, New York, 1970.
- [18] John Hubbard and Howard Masur. Quadratic differentials and foliations. *Acta Math.*, 142(3-4):221–274, 1979.
- [19] Yitzhak Katznelson. Ergodic automorphisms of  $\mathbb{T}^n$  are Bernoulli shifts. *Israel J. Math.*, 10:186–195, 1971.
- [20] Michael Keane and Meir Smorodinsky. Finitary isomorphisms of irreducible Markov shifts. *Israel J. Math.*, 34(4):281–286 (1980), 1979.
- [21] Maxim Kontsevich and Anton Zorich. Connected components of the moduli spaces of Abelian differentials with prescribed singularities. *Invent. Math.*, 153(3):631–678, 2003.
- [22] Jorge Lewowicz. Expansive homeomorphisms of surfaces. *Bol. Soc. Brasil. Mat. (N.S.)*, 20(1):113–133, 1989.
- [23] D. A. Lind. Dynamical properties of quasihyperbolic toral automorphisms. *Ergodic Theory Dynamical Systems*, 2(1):49–68, 1982.
- [24] Ricardo Mañé. Orbits of paths under hyperbolic toral automorphisms. *Proc. Amer. Math. Soc.*, 73(1):121–125, 1979.
- [25] Howard Masur. Interval exchange transformations and measured foliations. *Ann. of Math. (2)*, 115(1):169–200, 1982.
- [26] Howard Masur. Ergodic theory of translation surfaces. In *Handbook of dynamical systems. Vol. 1B*, pages 527–547. Elsevier B. V., Amsterdam, 2006.
- [27] Curtis T. McMullen. Dynamics of  $SL_2(\mathbb{R})$  over moduli space in genus two. *Ann. of Math. (2)*, 165(2):397–456, 2007.
- [28] Ja. G. Sinaĭ. Construction of Markov partitionings. *Funkcional. Anal. i Priložen.*, 2(3):70–80 (Loose errata), 1968.
- [29] William P. Thurston. On the geometry and dynamics of diffeomorphisms of surfaces. *Bull. Amer. Math. Soc. (N.S.)*, 19(2):417–431, 1988.
- [30] William A. Veech. Gauss measures for transformations on the space of interval exchange maps. *Ann. of Math. (2)*, 115(1):201–242, 1982.
- [31] Marcelo Viana. Ergodic theory of interval exchange maps. *Rev. Mat. Complut.*, 19(1):7–100, 2006.

- [32] Jean-Christophe Yoccoz. Continued fraction algorithms for interval exchange maps: an introduction. In *Frontiers in number theory, physics, and geometry. I*, pages 401–435. Springer, Berlin, 2006.
- [33] Anton Zorich. Explicit Jenkins-Strebel representatives of all strata of abelian and quadratic differentials. *J. Mod. Dyn.*, 2(1):139–185, 2008.